Sustainable Energy Future with Materials for Solar Energy Collection, Conversion, and Storage

Juvet Nche Fru, Pannan I. Kyesmen and Mmantsae Diale

1. Introduction

During the last 12 years, halide perovskites (HaP) have emerged as the fastest-emerging third-generation solar cell material, competing well with silicon and other thin-film technologies. The power conversion efficiency (PCE) of these easy-to-process and low-cost solar cells has risen from 3.58% to 25.6% from 2009 to 2021 (Zheng and Pullerits 2019; Jeong et al. 2021), already exceeding that of commercially available thin-film photovoltaics (PV) and rivaling that of the best single-junction silicon solar cells. Moreover, HaP have a wide range of applications including solar cells, water splitting and carbon dioxide (CO_2) reduction, light-emitting diodes, photodiodes in photodetectors, gas sensing, lasers and solar batteries. However, instability, toxicity of lead and solvents, poor laboratory-to-laboratory reproducibility, and scalability remain bottlenecks blocking the commercialization of this technology. Among all these difficulties, instability and short lifespan are the major impediments to the commercialization of HaP solar cells. It is crucial to understand the causes of instabilities and develop strategies that will stabilize this low-cost technology and facilitate its transfer to the market.

The production of solar hydrogen by water splitting through the PEC process was initially demonstrated by Fujishima and Honda in 1972 (Fujishima and Honda 1972). Fujishima and Honda used titanium dioxide (TiO_2) as a semiconductor photoanode and achieved a low quantum efficiency of 0.1%. A contributing factor to the low quantum efficiency was the inability of TiO_2 to absorb photons in the visible spectrum due to its large bandgap of 3.0 eV. The use of nitrides, chalcogenides, metal sulfides, and metal oxides as photoelectrodes for PEC water splitting has been explored for decades (Wang et al. 2017; Tee et al. 2017). Despite several decades spent in search of suitable materials, no single semiconducting material has been found to fulfill all the required performance benchmarks for efficiency, durability, and cost (Shen et al. 2014). Metal oxides are among the most promising candidates for use as photoanodes in PEC devices for hydrogen production. Their low cost, ease of

preparation, lattice manipulation flexibility, and stability in the PEC environment make them attractive (Eftekhari et al. 2017).

Popular metal oxide photoelectrodes for water splitting are TiO_2 (Eidsvåg et al. 2021), α-Fe_2O_3 (Kyesmen et al. 2021), bismuth vanadate ($BiVO_4$), and tungsten trioxide (WO_3) (Kafizas et al. 2017). Among these, α-Fe_2O_3 is a promising material for use as a photoelectrode in PEC water splitting due to its low bandgap, availability, low cost, non-toxicity, and stability in aqueous environments. It can absorb light in the visible region due to its bandgap of ~2.0 eV and promises a maximum theoretical photocurrent and solar-to-hydrogen (STH) efficiency of ~14 mA/cm^2 and ~17%, respectively (Dias et al. 2014; Murphy et al. 2006). In addition, α-Fe_2O_3 is the most common crystal structure of the oxides of iron, and it is easy to process (Yilmaz and Unal 2016). However, the efficiency of α-Fe_2O_3 is yet to attain the theoretically predicted value due to its poor conductivity, high electron–hole recombination, inefficient charge separation (Lee et al. 2014; Xi and Lange 2018), high overpotential, and low absorption coefficient, requiring films with a thickness of over 400 nm for sufficient photon utilization (Sivula et al. 2011). Numerous approaches have been employed in dealing with the challenges associated with the use of α-Fe_2O_3 for PEC water splitting. These strategies include nanostructuring (Ito et al. 2017), doping (Feng et al. 2020), formation of heterostructures (Natarajan et al. 2017), the use of co-catalysts (Eftekhari et al. 2017), plasmonic enhancement effects (Archana et al. 2015), and the use of light-harvesting bio-molecules (Ihssen et al. 2014).

In this chapter, we present the challenges of using HaP and α-Fe_2O_3 for the direct conversion of solar energy into electricity and hydrogen fuels, respectively, with a special focus on the up-to-date strategies that have been engaged towards overcoming them. The instability of perovskite solar cells is influenced by the Goldschmidt tolerance, chemical composition, and defects in halide perovskites. The use of additives to achieve large grain sizes with few grain boundaries and to passivate the surface and boundaries of HaP is effective in improving the stability of HaP solar cells. In addition, protecting back-metal contacts from reacting with the halide perovskites, passivation of 2D perovskites to form 2D/3D mixed-dimensional perovskites, encapsulation of the devices/modules, and use of MA-free perovskites as strategies for the long-term stability and lifetime of perovskite solar cells are presented. For α-Fe_2O_3 films, the simultaneous engagement of strategies such as nanostructuring, doping, formation of heterostructures, use of co-catalysts, and plasmonic enhancement effects has shown great promise in enhancing their photocatalytic hydrogen production. The concurrent use of multiple strategies for the enhancement of the solar-to-hydrogen conversion (STH) efficiency

of α-Fe$_2$O$_3$-based photoanodes is mostly implemented through the systematic use of interface engineering. More research is still needed to realize the anticipated commercialization of solar hydrogen production and photovoltaic technologies using α-Fe$_2$O$_3$ and halide perovskites, respectively.

2. Developments Towards Sustainability of Perovskite Solar Cells

2.1. Stability of Perovskite Solar Cells

Perovskite solar cells/panels in operation must withstand eternal environmental conditions including heat, moisture, oxygen, hail and external stresses such as heat/cold cycles, light/dark cycles. Stability can be regarded as the ability to maintain constant performance while operating under these conditions.

2.1.1. Goldschmidt's Tolerance Factor and Intrinsic Structural Stability of 3D HaP

Three-dimensional (3D) HaP solar cells are highly efficient but very unstable. In the AMX$_3$ form for 3D halide perovskites, A stands for a monovalent cation such as cesium (Cs$^+$), methylammonium (CH$_3$NH$_3{}^+$, MA), and formamidinium (H$_2$NCHNH$_2{}^+$, FA), M represents a divalent cation such as lead (Pb^{2+}) and tin (Sn^{2+}), and X is a halide anion such as bromide (Br$^-$), iodide (I$^-$), and chloride (Cl$^-$). Some 3D HaP have mixtures of the different A-cations, M-cations, and/or X-anions. The cubic perovskite crystal structure has an M-cation in the 6-fold coordination position, enclosed by a corner-linked octahedron of X-anions, called the MX$_6$ octahedral framework, and A-cations in the 12-fold coordination positions, as shown in Figure 1a. The size of the A-cation is larger than that of the M-cation, large enough to fit into the 12-fold coordinated voids of the MX$_6$ octahedral inorganic framework, to maintain the cubic symmetry, as shown in Figure 1b. HaP can reversibly transition between cubic, tetragonal, and orthorhombic crystal structures at different temperatures (Thomson 2018).

The ideal cubic symmetry of the 3D HaP structure is normally distorted in practice. Possible distortions include M-cation displacement from its central position and tilting of the MX$_6$ octahedron, depending on the sizes of the A-cation and M-cation. The degree of distortion is determined by Goldschmidt's tolerance factor (t), given by Equation (1),

$$t = \frac{\sqrt{2}\,(R_A + R_X)}{2\,(R_M + R_X)} \tag{1}$$

where R_A is the ionic radius of the A-cation, R_M is the ionic radius of the M-cation, and R_X is the ionic radius of the X-anion. It can also predict whether a combination of

anions and cations will form a stable HaP structure. For the ideal cubic symmetry, the ionic size requirement for stability is quite stringent, and the A-cation and M-cation adjust their equilibrium bond distances to the X-anions, without distortion of the unit cell, such that $t = 1$. The tolerance factor ranges from 0.8 to 1.0 for practical HaP because the cubic symmetry is distorted slightly to accommodate a wide range of cations and anions. For instance, the MX_6 octahedron may distort by tilting to reduce the coordination number from 12, so that a smaller sized A-cation can be accommodated, thereby decreasing t.
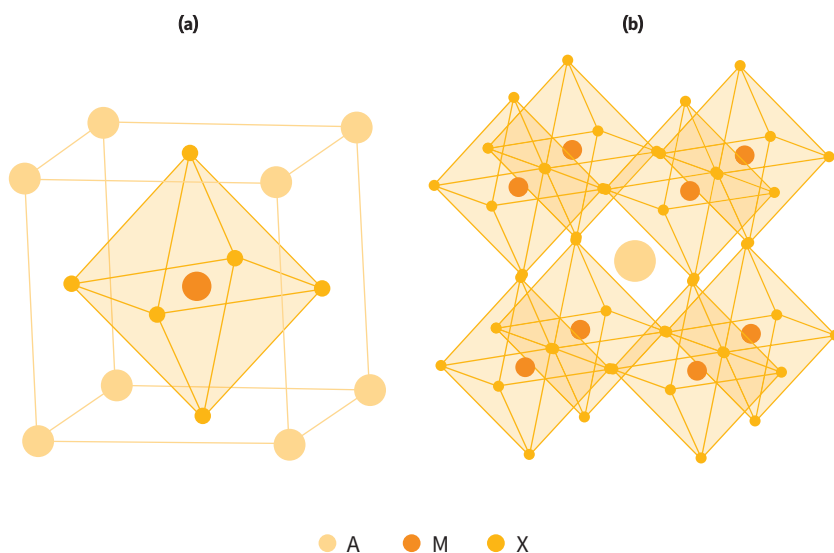

Figure 1. Cubic crystal structure (**a**) and A-Cation in 12-fold coordinated voids of the MX_6 octahedral inorganic framework (**b**) of HaP with general formula AMX_3. Source: Liu et al. (2015b).

2.1.2. Environmental/External Factors Responsible for the Degradation of HaP Solar Cells

Heat, light, moisture, oxygen and electrical bias, are among the environmental factors responsible for degradation of HaP. The action of light and heat on methylammonium lead tri-iodide may cause the evaporation of volatile components such as ammonia (NH_3) and iodine gas (I_2) (Juarez-Perez et al. 2018). As a result, the halide perovskite is irreversibly degraded/decomposed. Light soaking of HaP can cause negative effects such as ion migration (Zhao et al. 2017), halide segregation (Hoke et al. 2015), and photodecomposition (Kim et al. 2018).

2.1.3. Impact of Defects on the Stability of Perovskite Materials

The presence of defects in HaP reduces the charge carrier lifetime and impacts stability. Defects can be located at the interface between the active layers or in the bulk of the halide perovskites. These defects can be point (zero dimensional), line (one dimensional), surface (two dimensional), and volume (three dimensional) defects. Point defects in the widely studied MAPbI$_3$ include native defects such as positive iodine vacancies (I_V^+), negative iodine vacancies (I_V^-), neutral iodine vacancies (I_V), negative lead vacancies (Pb_V^{-2}), positive lead interstitials (Pb_i^{2+}), iodide interstitials (I_i), positive methylammonium interstitials (MA_i^+), negative methylammonium vacancy (MA_V^-), and impurities such as Au interstitials (Yang et al. 2016; Sherkar et al. 2017; Motti et al. 2019). Yang and co-workers (Yang et al. 2016) showed that the bulk I_V^+ have low formation energies, low diffusion barriers, and fast hopping rates, making them primarily responsible for ionic conductivity in MAPbI$_3$. They also showed that the diffusion barrier and formation energy of gold (Au) interstitial impurities in MAPbI$_3$ are low, leading to possible diffusion of Au into MAPbI$_3$ devices with biased Au/MAPbI$_3$ interfaces. Meanwhile, defects such as Pb_V^{-2}, Pb_i^{2+}, and MA_V^+ have very high activation energies, implying that their formation may require very high temperatures or strong irradiation conditions to form, thus not likely participating in the defects (Motti et al. 2019). Cation substitutions such as MA_{Pb} and Pb_{MA} and substitution anti-sites including MA_I, Pb_I, I_{MA}, and I_{Pb} are also present in MAPbI$_3$ (Jin et al. 2020; Yang et al. 2017b). The nature of Schottky defects and Frenkel-type defects has also been studied in HaPs. Dewinggih and co-workers (Dewinggih et al. 2017) showed that iodine vacancy/interstitial (I_V^+/I_V^-) Frenkel pair trapping centers are abundant in MAPbI$_3$ and are annihilated under illumination conditions which increases photoluminescence quantum efficiency. Kim and co-workers (Kim et al. 2014) showed that the formation energies of Schottky defects (neutral vacancy pairs) such as PbI$_2$ and MAI in MAPbI$_3$ are relatively low. Fortunately, these defects are not trap states that can reduce the carrier lifetime. A Schottky couple in HaP has very low formation energies and originates from halide vacancy coupling with the metal vacancies (Motti et al. 2019).

Planar defects include grain boundaries (GBs), surfaces or perovskite/transport layer interfaces, stacking faults, and twin boundaries. GBs are interfaces between two grains in polycrystalline materials, as shown in Figure 2a. It has been shown that degradation in HaP starts at the surface and grain boundaries (Shao et al. 2016). This is because GBs are sources of high defect densities, trap accumulation sites, infiltration sites for water vapor, and fast pathways for ion migration due to reduced steric hindrance (Shao et al. 2016). Grain boundaries absorb moisture

and oxygen from the environment and cause HaP degradation (Wu et al. 2021). The transformation of the perovskite phase to a non-perovskite phase is initiated at boundaries which are active sites accumulating chemical species (Yun et al. 2018). GBs serve as trapping centers for charge carriers, leading to non-radiative recombination that reduces the carrier lifetime, and also causing hysteresis in the current–voltage characteristic (Uratani and Yamashita 2017). DeQuilettes and co-workers (DeQuilettes et al. 2015) measured the photoluminescence intensities and carrier lifetimes from different grains and grain boundaries of the same $MAPbI_3$ thin film. They concluded that grain boundaries are dimmers and show the fastest non-radiative recombination. The surfaces of HaP are also defective, as shown in Figure 2b. They contain a large number of charged defects (Zhang et al. 2019b) including iodine vacancies (Wu et al. 2020), X-terminating surfaces with nonstoichiometric compositions (Qiu et al. 2020), and improper bonding: (110)-X_2 halide surfaces with a large number of broken bonds (Jain et al. 2019; Kong et al. 2016), and Pb dangling bonds (Kong et al. 2016). SRH recombination at interfaces with the transport layers is the dominant loss mechanism in perovskite solar cells (Sherkar et al. 2017). With regard to stacking faults, they occur in crystals characterized by a periodic sequence of atomic planes due to an interruption in the typical regular arrangement. Song and co-workers (Song et al. 2015) showed that $MAPbI_3$ phases with I/Pb ratios ranging from 3.2 to 3.5 form stacked perovskite sheets with a large amount of stacking faults, whereas thin films with I/Pb ratios ranging from 2.9 to 3.1 form the conventional 3D perovskite with few stacking faults (alpha phase). First principle studies of the electronic properties of {111} twin boundaries in mixed HaP containing FA, Cs, Br, and I revealed that twin boundaries in these perovskites are nucleation sites for I-rich and Cs-rich formation, which are hole traps and can cause electron–hole recombination, leading to a loss in V_{oc} (Mckenna 2018). Direct imaging using TEM has revealed twin boundaries in a $MAPbI_3$ thin film range from 100 to 300 nm wide with twin boundaries parallel to {112}$_t$ (Rothmann et al. 2017). By varying the anti-solvent during deposition, Tan and co-workers (Tan et al. 2020) were able to change the defect density of the (111) twin boundary for $Cs_{0.05}FA_{0.81}MA_{0.14}PbI_{2.55}Br_{0.45}$ mixed perovskite to establish the relationship with PCE. It has been shown that recombination centers limiting charge carrier lifetimes in HaP are preferentially located close to the surface rather than in the bulk of the crystal (Stewart et al. 2016).
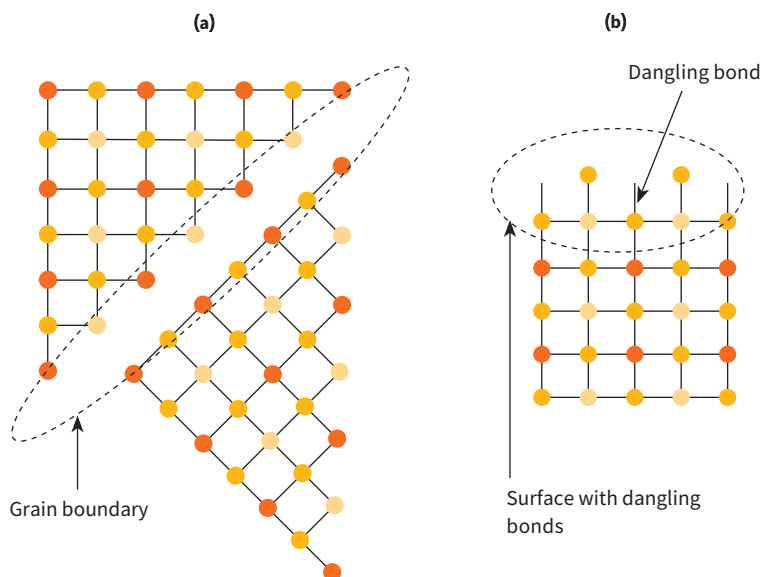
Figure 2. Schematic diagram showing grain boundaries (**a**) and surface defects (dangling bonds) (**b**) in HaP. Source: Graphic by authors.

2.1.4. The Reaction of HaP with Metal Back-Electrodes

Another primary source of instability is caused by the reaction of HaP with widely used metal electrodes when in direct or indirect contact. Gold (Au), silver (Ag), and copper (Cu) are widely preferred as back-electrodes in perovskite solar cells due to their high conductivity. Indirect contact occurs when the metal diffuses through the hole and electron transport layers into the active layer of the device and reacts with the perovskite to form insulating metal halide species or defect states in the bulk or at the surface (Domanski et al. 2016), reducing the thermal stability of the device (Boyd et al. 2018; Domanski et al. 2016). Halide can also diffuse out of the active layer and make contact with the electrodes. For instance, corrosion of a silver (Ag) electrode due to the reaction with diffused hydrogen iodide (HI), produced during the decomposition of a MAPbI$_3$ absorber of an encapsulated solar cell, has been shown to speed up the degradation of MAPbI$_3$ (Han et al. 2015). Wang and co-workers (Wang et al. 2018) showed that MAPbI$_3$ reacted rapidly with Ag electrodes, and the reaction was driven by diffused iodide (I$^-$) ions which caused corrosion of the electrode. Gold electrodes corrode rapidly due to the aggressive chemical interaction between gold and highly reactive iodine-containing by-products formed in the course of perovskite decomposition under illumination with intense

UV radiation (Shlenskaya et al. 2018). In addition, metal electrodes can diffuse into the HaP active layer through the hole transport layer or electron transport layer, leading to degradation of the perovskite (Ming et al. 2018; Zhao et al. 2016b). In $CH_3NH_3PbI_3$ devices with Al electrodes and the presence of moisture, Al rapidly reduces Pb^{2+} to Pb^0 and converts $CH_3NH_3PbI_3$ to $(CH_3NH_3)_4PbI_6 \cdot 2H_2O$ and then to CH_3NH_3I (Zhao et al. 2016b).

Electrodes are deposited directly on perovskite in hole conduction layer-free solar cells (Asad et al. 2019). The perovskites are deposited directly on metal electrodes in cells without charge transport layers (Lin et al. 2017). Metal electrodes also make direct contact with HaP in Schottky diodes, resistive switching devices, and photodetectors. The electrodes of Schottky diodes, resistive switching devices, and photodetectors also directly contact HaP (Li et al. 2019; Kang et al. 2019). Halide perovskite becomes unstable when in direct contact with metal electrodes. We have shown that methylammonium lead tri-bromide ($MAPbBr_3$) perovskite grains delaminate rapidly on Al-coated substrates as opposed to Au, Ag, Au-Zn, and Sn substrates (Fru et al. 2021). The direct contact of Ag with perovskites also speeds up their degradation, leading to a loss in organic cations (Svanström et al. 2020). These results are important in the selection of electrodes for stable charge transport layer-free solar cells.

2.2. HaP Panel/Module Lifetime

A sustainable transfer of the perovskite solar cell technology from the laboratory to market requires the module/panel lifetime to be greater than 20 years. A widely used definition of module lifetime, known as the T_{80} lifetime, is the time taken for its efficiency to decrease by 20% of the initial value (He et al. 2020). The failure of a module in photovoltaic technology is determined using the T_{80} lifetime. The T_{80} lifetime is calculated using Equation (2),

$$T_{80} = \frac{20\%}{Degrad_{rate}} \tag{2}$$

The median degradation rate ($Degrad_{rate}$) of commercially available solar modules ranges from 0.36%/year for monocrystalline silicon to 0.96%/year for copper indium gallium selenide (CIGS), providing T_{80} lifetimes of over 55.6 and 20.8 years, respectively. These degradation rates were determined from a field test with solar modules operating under normal working conditions. However, the average degradation rate of perovskite solar modules is 66%/year, corresponding to an average lifetime of 0.30 years (3.6 months). These results indicate that perovskite solar

modules are very unstable under real operating conditions, and intensive research is needed to commercialize the technology. The lifetime of a solar panel/module is highly correlated with the stability of the constituent solar cells.

2.3. Improving the Stability of Perovskite Solar Cells/Panels

Various strategies have been employed to improve the stability of perovskite solar cells. These techniques can be grouped into stable materials synthesis, additives and passivation, alternative robust functional layers, encapsulation, and engineering of 2D and 2D/3D mixed-dimensional perovskites.

2.3.1. Towards Compositional Stability 3D Halide Perovskite Materials

Degradation due to light and heat is mitigated by improvement in the HaP material and interfaces of the solar cell. Careful selection of the organic cation in HaP is necessary to prevent irreversible degradation (decomposition) under the action of heat and light (Juarez-Perez et al. 2018). This decomposition is mainly due to the release of volatile components in MA-containing perovskites. Thus, it has been shown that going MA free will produce inherently stable perovskites (Turren-Cruz et al. 2018). An alternative organic cation for 3D HaP is formamidinum (FA). The high enthalpy and activation energy needed for its decomposition make FA more resistant to thermal decomposition and produce more thermally stable perovskites than MA (Juarez-Perez et al. 2019). However, FA-based perovskites lack phase stability under humidity and thermal stress (Chen et al. 2021). Much effort is being directed towards the stabilization of the black phase of FA-based perovskites through additives, doping, alloying, interfacial engineering, etc. (Chen et al. 2021). The use of a low-vapor pressure inorganic cation such as cesium (Cs) as a substitute for high-vapor pressure MA leads to a more stable completely inorganic HaP. By mixing the A-site cations, composition stability can also be achieved.

2.3.2. Additives and Passivation

Figure 3a,b show the schematic diagrams of defective and passivated surfaces. Most attempts to mitigate these surface defects involve using different additives that will either improve the film morphology by increasing the grain size to reduce the number of grain boundaries or cause surface passivation (Zhang et al. 2016a). Passivation can be conducted by using various additives including small molecules (Xu et al. 2016), polymers (Dunn et al. 2017), ligands (Zhang et al. 2019a), perovskite quantum dots (Zheng et al. 2019), and 2D perovskites (Rahmany and Etgar 2021). The effect of grain boundaries on the lifetime of charge carriers has

been reduced by passivation of the perovskite surface with Lewis acid additives such as 1,2-ethanedithiol (Stewart et al. 2016) and Lewis base additives (Noel et al. 2014). These studies suggested that the Lewis bases donate electrons to surface traps, thus preventing them from capturing charge carriers, while the Lewis acids donate protons, as shown in Figure 3b. Surface treatment by post-deposition of a variety of Lewis bases (electron-donating molecules) and surface ligands passivates surface defects, thereby reducing non-radiative recombination. The presence of excess PbI_2 between grain boundaries also has a passivation effect (Chen et al. 2014). The addition of an optimum amount of potassium iodide (KI) in triple-cation $(Cs_{0.06}FA_{0.79}MA_{0.15})Pb(I_{0.85}Br_{0.15})_3$ perovskite reduces non-radiative losses and photoinduced halide ion migration by passivation of the perovskite film and interfaces (Abdi-jalebi et al. 2018). This is achieved by the excess iodide from KI compensating for any halide vacancies (trap states). At the same time, potassium ion selectively depletes bromide from the crystal, thereby reducing trap states that result from bromide-rich perovskites. The formation of benign (potassium-rich, halide-sequestering species) from excess halides at the grain boundaries and interfaces immobilizes halide ion migration. The addition of a strong electron acceptor of 2,3,5,6-tetrafluoro7,7,8,8-tetracyanoquinodimethane (F4TCNQ) into the perovskite functional layer fills grain boundaries, thus reducing metallic lead defects and iodide vacancies significantly (Liu et al. 2018). Excess MAI intrinsically passivates the surface of $MAPbI_3$ films, leading to a reduced surface recombination velocity and an improved total carrier lifetime (Yang et al. 2017a). Additives such as sulfonated carbon nanotubes (Zhang et al. 2016a), Lewis bases such as urea and thurea (Hsieh et al. 2018), and Lewis acid−base adducts (for example, the PbI_2 adduct with the O-donor DMSO is excellent for improving grain size in $MAPbI_3$ and PbI_2 adducts, while the S-donor thiourea is excellent for $FAPbI_3$) (Lee et al. 2015) mitigate defects by producing larger grains with fewer grain boundaries. The addition of sulfonated carbon nanotubes also passivates perovskite by filling grain boundaries (Zhang et al. 2016a). Other Lewis bases such as thiophene and pyridine passivate the perovskite surface by donating an electron to under-coordinated Pb atoms present in the crystal (Noel et al. 2014). Fullerenes (PCBM) deposited on the top of the perovskite have a passivation effect which reduces photocurrent hysteresis and the trap density (Shao et al. 2014). Fang and co-workers (Fang et al. 2020) showed that the 4-fluorophenylmethylammonium-trifluoroacetate additive passivates both uncoordinated lead and halide ions in the mixed-cation mixed HaP $FA_{0.33}Cs_{0.67}Pb(I_{0.7}Br_{0.3})_3$. This is possible because the trifluoroacetate anion binds with the lead cation, and the 4-fluorophenylmethylammonium cations bind with the

halide ion. This dual passivation suppressed hysteresis, halide segregation, and ion migration, leading to an improvement in the operational lifetime of light-emitting diodes from 1.0 to 14.0 h. Qiao and co-workers (Qiao et al. 2019) showed that alkali metals mitigate I_i defects in two ways: by increasing their formation energy, thus reducing their concentration, and binding strongly to them, thereby eliminating mid-gap states that act as traps for electrons and holes, thus increasing the carrier density and extending the carrier lifetimes significantly.
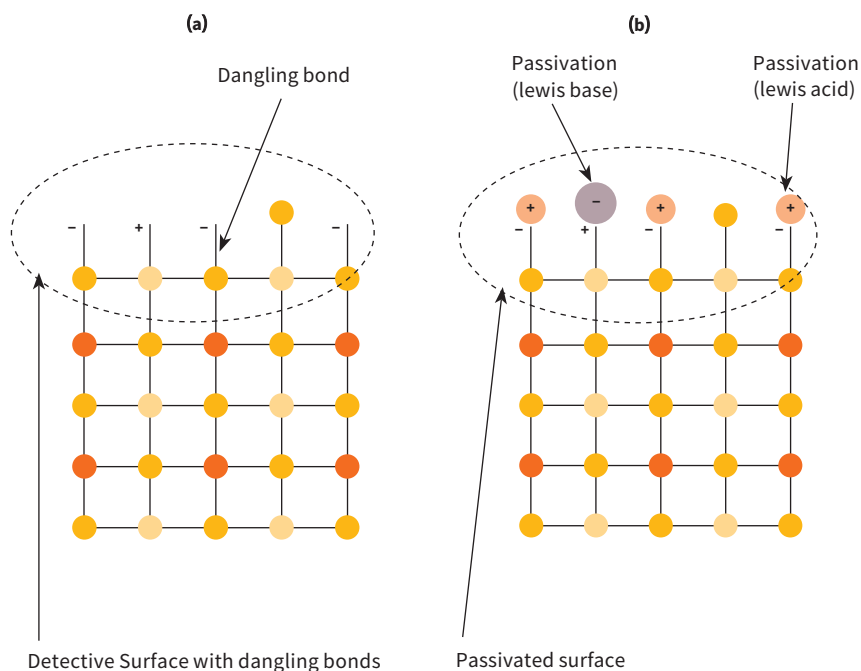
Figure 3. The schematic diagrams of defective (**a**) and passivated (**b**) surfaces. Source: Graphic by authors.

2.3.3. Encapsulation

Encapsulation is an important method to solve instability problems, prevent the leakage of toxic and water-soluble lead compounds to the environment, and help the perovskite solar module to pass the hail impact test (He et al. 2020). In addition, it prevents contact with ambient air, prevents leakage of volatile components, and reduces moisture and heat degradation. Table 1 describes various techniques and materials for encapsulating HaP solar cells. High-performance encapsulation materials should be easy to process and chemically inert and have

a low oxygen transmission rate, low water vapor transmission rate, high dielectric constant, resistance to UV and thermal oxidation, high adhesion to perovskite solar modules, similar coefficients of thermal expansion to perovskite solar cell materials, and high mechanical impact strength (Griffini and Turri 2016; Aranda et al. 2021). The techniques used for perovskite solar cells include rigid glass–glass encapsulation, ultra-thin flexible glass sheet encapsulation, polymeric laminates, thin-film barrier-coated webs, and thin-film encapsulation (TFE).

Table 1. Summary of encapsulation methods and materials.

Encapsulation Method	Description	Materials
Glass–glass encapsulation (rigid, widely used, straightforward, very effective, very affordable, incompatible with flexible devices)	The device is sandwiched between two rigid glass sheets using thermo-curable adhesives or UV-curable sealants. Edges are sealed with sealants to prevent ingress of oxygen and moisture.	Examples of thermo-curable adhesives include ethylene-vinyl acetate (EVA) (Bush et al. 2017), surlyn ionomer (Cheacharoen et al. 2018), and polyisobutylene (PIB) (Shi et al. 2017). UV-curable adhesives include epoxy resin (Mansour Rezaei Fumani et al. 2020; Ierides et al. 2021). Edge sealants include butyl rubber and PIB (Vidal et al. 2021).
Ultra-thin flexible glass sheet encapsulation (most recent, flexible, high cost, effects on performance and long-term stability, needs investigation)	Flexible device sandwiched between ultra-thin flexible glass sheets.	Hermetic glass frit (Fantanas et al. 2018; Emami et al. 2020).
Polymeric laminates and thin-film barrier-coated webs (used for both flexible and rigid solar cells)	Can be used as substrates in flexible solar cells and as an encapsulating agent on various types of substrates.	Poly(methylmethacrylate) (PMMA), polyethylene terephthalate (PET), polydimethylsiloxane (PDMS), polyethylenenaphthalate (PEN).
Thin-film encapsulation (TFE) (emerging and promising, expensive, challenging)	Direct deposition of a single ultra thin-film flexible protective layer on the device using vacuum deposition methods including physical vapor deposition, chemical vapor deposition, plasma-enhanced chemical vapor deposition, and atomic layer deposition.	Metal oxides including Al_2O_3, SiO_x, TiO_2, and Zn_2SnO_4 (Aranda et al. 2021). Multilayer stacked organic/organic layers called dyads (Lee et al. 2018) and ultra-thin plasma polymeric films (Idígoras et al. 2018).

Source: Table by authors.

2.3.4. 2D and 2D/3D Mixed-Dimensional Perovskites

Two-dimensional HaP have layered structures that are similar to the Ruddlesden–Popper (RP) phases (Ruddlesden and Popper 1958), consisting of a nanoplatelet (nanosheet) perovskite that is separated by large spacer cations. The RP phase has the general formula $A_{n-1}L_2M_nX_{3n+1}$. In this form, A is a small-size monovalent cation (Cs^+, MA^+), L corresponds to a large-size aromatic or aliphatic alkylammonium spacer cation including phenyl-ethyl ammonium (PEA^+) and butylammonium (BA^+), M is a transition metal cation (such as Pb^{2+} and Sn^{2+}), X stands for a halide anion (such as I^-, Br^-, and Cl^-), and the integer n represents the number of metal halide octahedral $[MX_6]^{4-}$ layers between the two L-cations, determined by careful control of the stoichiometry (Shi et al. 2018). Two-dimensional perovskites have strong quantum confinement effects and large bandgaps (Zhang et al. 2020). In solar cells, 2D perovskites have been applied as primary light harvesters (Cao et al. 2015), capping layers (Chen et al. 2018), passivation layers (Jiang et al. 2019), and 2D/3D interfacial layers (Niu et al. 2019). Two-dimensional HaP solar cells are more stable than their 3D counterparts but less efficient. Moreover, their hydrophobicity and moisture resistance improve device stability under high humidity (Zheng et al. 2018).

Two-dimensional/three-dimensional mixed-dimensional perovskite solar cells combine the stability of 2D perovskites with the excellent light-harvesting properties of 3D perovskites to produce stable and efficient devices. When grown on 3D perovskites to form a 2D/3D mixed-dimensional perovskite, grain boundaries and surface charged defects are passivated to enhance stability (Wu et al. 2021). In 2017, Grancini et al. (2017) obtained a stable 10 cm × 10 cm perovskite solar cell that maintained its 11.6% PCE for more than 10,000 h under controlled standard conditions using a fully printable industrial process. Remarkable stability was achieved through 2D/3D interface engineering in which the 2D layer prevented moisture ingress.

2.3.5. Use of Stable Metal Electrodes and Very Thin Interlayers

As explained above, diffusion of the widely used Au, Al, Ag, and Cu electrodes into the HaP active layer is one of the leading causes of instability. Very thin barrier layers including chromium (Domanski et al. 2016), chromium oxide-chromium (Cr_2O_3/Cr) (Kaltenbrunner et al. 2015), MoO_x (Sanehira et al. 2016), bismuth (Bi) (Wu et al. 2019), and amine-mediated titanium suboxide ($AM\text{-}TiO_x$) (Back et al. 2016) have been employed between the perovskite and hole transport layers to protect metal top contacts from reaction with the halide perovskites. Domanski et al. (2016) showed

that, at 70 °C, gold (Au) diffused through the HTL into the HaP layer. However, the diffusion was prevented by depositing a layer of chromium (Cr) between the HTL and the Au electrode. The Cr layer alleviated the severe degradation of the device performance at elevated temperatures. In comparison to Au and Ag, Cu electrodes do not diffuse into the perovskite active layer and produce more stable perovskite solar cells (Zhao et al. 2016a). Zhao et al. demonstrated that high-PCE Cu electrode-based solar cells with efficiency above 20% retain 98% of the initial PCE after 816 h of storage in an ambient environment without encapsulation (Zhao et al. 2016a). Cu and Ag do not form deep-level trap states in $MAPbI_3$-based solar cells (Ming et al. 2018). Additionally, the conventional noble metal electrodes are not sustainable because of the cost, scarcity, and complexity of metal ore extraction. To overcome these problems, carbon electrodes are gaining increased attention due to their low cost, excellent stability, and compatibility with up-scaling techniques. However, ultra-thin buffer layers of materials such as Cr are required between the electrode and the charge transport layers to ensure good electrical contact (Babu et al. 2020).

3. Solar Hydrogen Production

PEC water splitting, a technology for solar hydrogen production, is an attractive approach for numerous reasons. First, photocatalytic hydrogen production offers an attractive route for solar energy storage. This is because hydrogen energy storage has been considered as the most suitable means for storing excess off-peak power where long-term storage is a priority (Benato and Stoppato 2018). In addition, hydrogen can be easily transported via land, air, or sea, making it possible to transport solar energy (converted to hydrogen) from one geographical location to another. Additionally, hydrogen fuel already has a vast and established economy with numerous applications in homes and industries. Hydrogen can be converted directly into electricity for domestic consumption, use for the powering of automobiles, and as fuel in the aviation industry (Glanz 2010). The numerous applications of hydrogen make its production from solar energy more attractive considering the global need for clean energy production for a sustainable future.

The device used for harvesting solar energy for photocatalytic hydrogen production is often known as a PEC cell (Figure 4). The basic operation of a PEC device has been reported by many authors (Glanz 2010; Ihssen et al. 2014). Here, a summary of the operation of a PEC cell is explained using a device consisting of a photoanode and a metallic counter electrode immersed in an acidic electrolyte. Equation (3) presents an illustration of the basic operation of a PEC device for water

splitting. First, the photoanode will absorb photons when irradiated with incident photon energy hv and become ionized, resulting in the generation of electron–hole pairs. If recombination does not occur, the hole (h^+) becomes separated from the electron (e^-), moves to the surface of the photoanode, and oxidizes water to produce oxygen gas and H^+ ions, as shown in Equation (1). The H^+ ions produced at the surface of the photoanode are transported to the cathode. Simultaneously, the electrons produced in the photoanode are driven to the cathode through the external circuit where they interact with the H^+ ions to produce H_2 gas, as shown in Equation (4). The chemical reaction for the decomposition of water into O_2 and H_2 via PEC water splitting is summarized in Equation (5). Examples of materials that could be used as a photoanode in PEC devices include n-type semiconductors such TiO_2, $BiVO_4$, and α-Fe_2O_3.
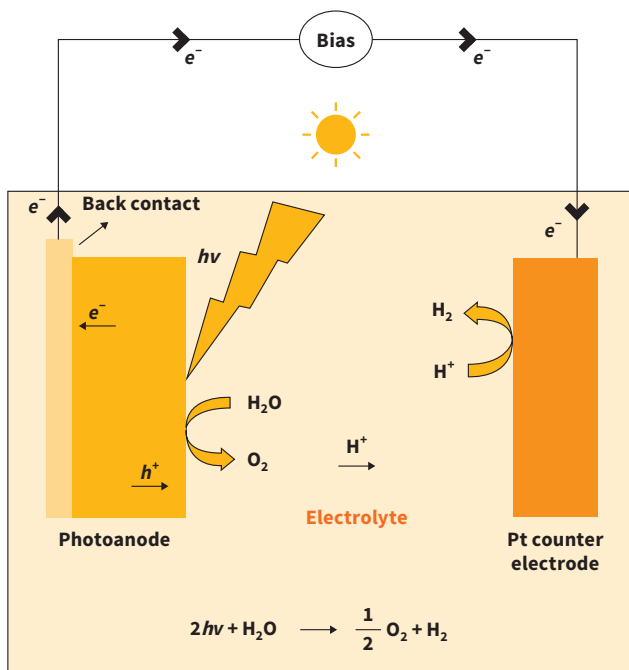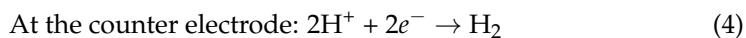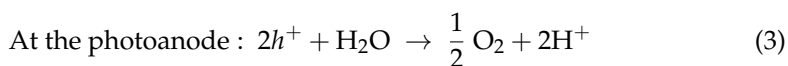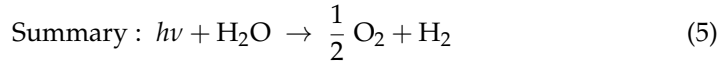

Figure 4. Schematic illustration of the basic operation of a PEC device. Source: Graphic by authors.

$$\text{At the photoanode}: \ 2h^+ + H_2O \ \rightarrow \ \frac{1}{2} O_2 + 2H^+ \tag{3}$$

$$\text{At the counter electrode}: 2H^+ + 2e^- \rightarrow H_2 \tag{4}$$

$$\text{Summary}: h\nu + H_2O \; \rightarrow \; \frac{1}{2}\,O_2 + H_2 \qquad\qquad (5)$$

3.1. Hematite as Photocatalyst

Hardee and Bard were the first to use a hematite photoelectrode for water photolysis in 1976 (Cattarin and Decker 2009). The stability of hematite in an aqueous environment and its ability to absorb photons in the visible region are the major properties that have continued to attract increased research into its application in PEC water splitting. An increasing amount of research is still being channeled towards overcoming the major challenges inhibiting the use of hematite as a photoanode in solar hydrogen production. The main challenges are outlined in Section 1, which include its poor conductivity, high electron–hole recombination, and inefficient charge separation, among others. The strategies which have been developed over the years towards overcoming the problems that have been limiting the application of hematite-based photoanodes in solar hydrogen production are discussed in the following section.

3.2. Strategies for Enhancing the PEC Properties of α-Fe_2O_3 Films

3.2.1. Nanostructuring

Nanostructuring is the fabrication of materials consisting of structural features in the nanometer scale (Singh and Terasaki 2008). Nanostructured materials provide flexible space for ease of fabrication, enhanced mechanical stability, confinement effects, and a large surface area, making them suitable for photocatalytic applications (Rani et al. 2018). The nanostructuring approach has long been employed in the fabrication of α-Fe_2O_3 thin films to mitigate their poor charge transport property without compromising their photon absorption for PEC applications. α-Fe_2O_3 has a low absorption coefficient and, as a result, requires films of 400–500 nm thickness for complete light absorption. Because of the short hole diffusion length of 2–4 nm (Ahn et al. 2014), photogenerated charge carriers in bulk α-Fe_2O_3 films will likely recombine before reaching the surface of the films to perform water oxidation, which will result in a low photocurrent in the PEC device. Since thinner α-Fe_2O_3 films are not able to absorb sufficient photons for a significant photocatalytic activity, nanostructuring has been employed to help solve this paradox. Nanostructured α-Fe_2O_3 films that can absorb sufficient photons can also offer a large interfacial area for interaction with the electrolyte, making them suitable for promoting charge carrier transport during photocatalytic reactions (Tamirat et al. 2016; Annamalai et al. 2016).

The nanostructuring approach has been widely utilized in preparing α-Fe$_2$O$_3$ films of different morphologies and has been shown to help promote charge separation on the film's surfaces where water oxidation/reduction reactions occur during photocatalysis (Annamalai et al. 2016). Nanostructured α-Fe$_2$O$_3$ films with morphologies such as nanoparticles (Souza et al. 2009), nanorods (Ito et al. 2017), nanoflowers (Tsege et al. 2016), nanocones (Li et al. 2014), nanosheets (Peerakiatkhajohn et al. 2016), nanotubes (Kim et al. 2016a), and nanowires (Xie et al. 2018; Grigorescu et al. 2012) have been prepared for PEC water splitting, yielding an improved photocurrent density compared to the bulk films (Chou et al. 2013). Figure 5 presents a schematic illustration for some of the different morphologies of hematite films for PEC water splitting. One of the major limitations of nanostructuring is its inability to influence the intrinsic properties of hematite such as its low electrical conductivity of 10^{-14} Ω^{-1} cm^{-1} (Tamirat et al. 2016) and charge carrier lifetime of 3–10 ps (Grave et al. 2018).
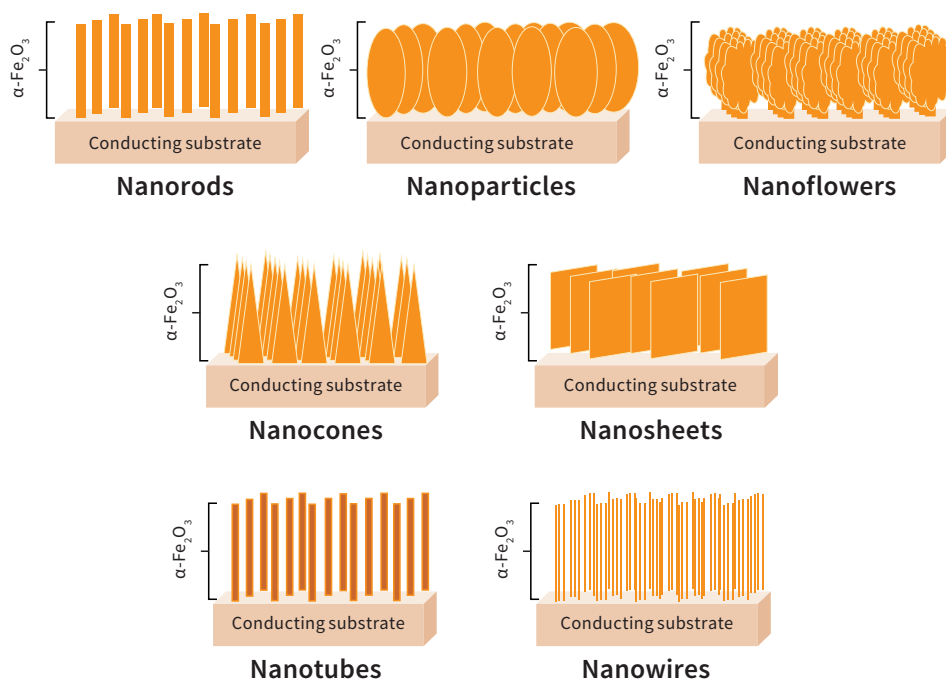

Figure 5. Schematic illustration of different morphologies of hematite films for PEC water splitting. Source: Graphic by authors.

3.2.2. Doping

The introduction of impurities into a semiconductor, termed doping (Grundmann 2010), can positively alter its intrinsic properties for PEC applications. Doping of semiconductor materials can help to narrow their optical bandgap and influence electrical properties, such as an increase in the charge carrier's concentration and mobility, thereby improving PEC performance (Yang et al. 2019). For α-Fe_2O_3, elemental doping involves replacing the lattice iron with foreign atoms, in order to influence its intrinsic properties for improved photocatalytic capability. The intrinsic properties of α-Fe_2O_3 which negatively affects its efficacy in PEC devices such as its low electrical conductivity of 10^{-14} Ω^{-1} cm^{-1}, charge carrier concentration on the order of 10^{18} cm^3, electron mobility of 10^{-2} cm^2 V^{-1} s^{-1}, hole mobility of 0.0001 cm^2 V^{-1} s^{-1}, and charge carrier lifetime of 3–10 ps have been improved through doping (Tamirat et al. 2016; Grave et al. 2018). Doping can significantly cause an increase in the charge carrier concentration in hematite films which directly improves their conductivity. Both experimental evidence (Gurudayal et al. 2014; Mao et al. 2011) and theoretical calculations (Zhang et al. 2016b) have confirmed the enhancement of the charge carrier concentration through doping. In addition, enhancement of the photocatalytic capabilities of hematite through doping has also been associated with the passivation of surface states and grain boundaries, shifting of band edge positions, and the distortion of its crystal structure which facilitates charge carrier hopping and transport (Grave et al. 2018).

The PEC performance of α-Fe_2O_3 films has been improved through doping with n-type dopants such as Ti (Feng et al. 2020; Peng et al. 2021), Pt (Mao et al. 2011), and Sn (Li et al. 2017), p-type dopants such as Mn^{2+} (Gurudayal et al. 2014), Cu^{2+} (Tsege et al. 2016), and Ag^+ (Shen et al. 2014) [4], and non-metals such as Si (Dias et al. 2014), S (Bemana and Rashid-Nadimi 2017), and P (Zhang et al. 2015). Feng et al. (2020) achieved an over 2-fold increment in the photocurrent density at 1.23 V vs. RHE and a negative onset potential shift of over 200 mV for α-Fe_2O_3 photoanodes through Ti doping. They attributed the improved PEC water splitting to an increase in the charge carrier density and enhanced charge separation. Elsewhere, a 3-fold increase in the photocurrent density was achieved for α-Fe_2O_3 nanorods through p-type doping with Mn, and the onset potential shifted by 30 mV to a more negative value. The boost in PEC water splitting was also associated with the increased charge carrier density as well as the reduced electron–hole recombination rate in Mn-doped α-Fe_2O_3 photoanodes (Gurudayal et al. 2014). In another study, a photocurrent density of 1.42 mA/cm^2 at 1.23 V vs. RHE was achieved for S-doped α-Fe_2O_3 nanorods, representing a 4-fold increase compared to the undoped films. The authors

attributed the superior PEC activity to the improved charge carrier mobility of the S-doped α-Fe$_2$O$_3$ films (Zhang et al. 2017).

3.2.3. Heterojunction Formation

The heterojunction architecture involves the coupling of two semiconducting materials to improve PEC water splitting efficiency. Depending on the semiconductor materials used to form the heterostructure (*n*-type or *p*-type), *n–n*, *p–p*, or *p–n* junction structures could be formed. Heterojunction formation confers three major contributions: enhanced visible light absorption, improved charge separation, and increased lifetime of charge carriers (Tamirat et al. 2016). Heterojunction structures allow for the incorporation of materials of different bandgaps, broadening the photon absorption spectrum of the heterostructure for better photocatalysis (Mayer et al. 2012; Sharma et al. 2015; Kyesmen et al. 2021). Additionally, the formation of a heterojunction results in the development of an internal electric field at the space charge region between the heterostructures which helps in facilitating charge carrier transport. This will culminate in improving charge separation and increasing the carrier lifetime, leading to reduced electron–hole recombination and enhanced PEC efficiency during water splitting (Bai et al. 2018; Selim et al. 2019).

The charge transport mechanism and energy band diagram of hematite-based photoanodes during PEC water splitting can be explained using the *p–n* heterojunction structure presented in Figure 6. When a heterojunction is formed between two semiconductors, a space charge layer is created at the interface between them. For a *p–n* heterojunction with a hematite-based photoanode, the valence band (VB) and conduction band (CB) edges of the p-type semiconductor material both need to be more negative than those of α-Fe$_2$O$_3$ (Afroz et al. 2018). Additionally, the electrons from the CB of the p-type semiconductor are transferred to the CB of α-Fe$_2$O$_3$ and then to the fluorine-doped tin oxide (FTO) substrate, where they move onto the counter electrode through the back-contact to reduce H$^+$ to H$_2$. The movement of photogenerated charge carriers across the heterojunction is facilitated by the electric field formed at the interface between the composite materials, enhancing the effective charge separation and reducing the recombination rate of electron–hole pairs (Liu et al. 2015a). For an *n–n* heterojunction-structured hematite-based photoanode, a similar operation mechanism and energy band bending to those of the *p–n* junction apply. However, the semiconductor material is required to have more negative CB and VB band positions relative to those of hematite.
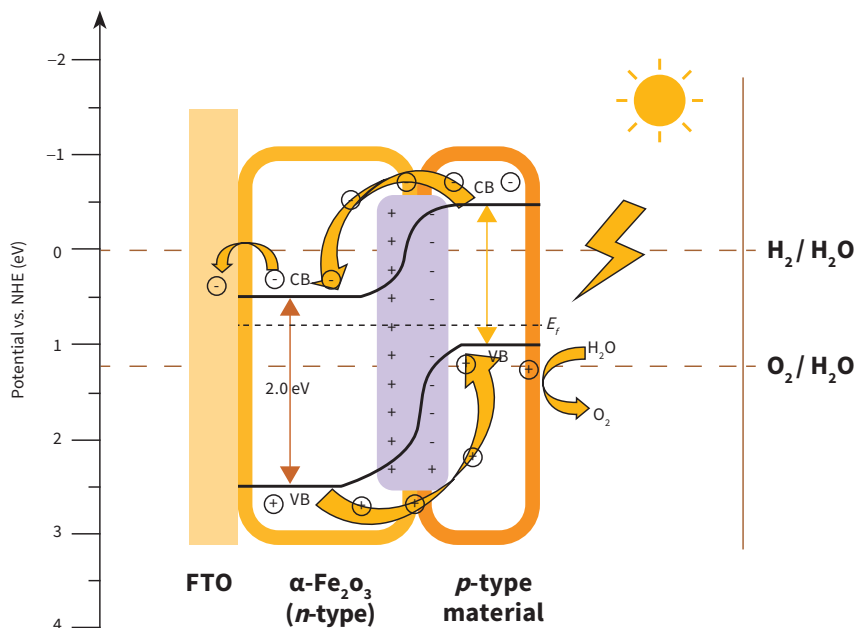
Figure 6. The charge transport mechanism and energy band diagram of the hematite-based *p–n* heterojunction structure during PEC water splitting. Source: Graphic by authors.

Furthermore, different composite materials have been employed in improving the PEC water splitting of α-Fe$_2$O$_3$. The formation of the α-Fe$_2$O$_3$/NiO heterojunction structure has been reported to improve the photocurrent density of α-Fe$_2$O$_3$ from 0.042 to 0.156 mA/cm^2 at 0.4 V vs. AgCl. The improvement was attributed to the enhanced charge transfer kinetics resulting from the formation of the α-Fe$_2$O$_3$/NiO heterostructure (Bemana and Rashid-Nadimi 2019). Natarajan et al. (2017) fabricated α-Fe$_2$O$_3$/CdS heterostructures and achieved a photocurrent density of 0.6 mA/cm^2 at 0.92 V vs. RHE and a 0.4 V negative shift in the onset potential compared to the value recorded for pristine α-Fe$_2$O$_3$ films. They attributed the enhancement in PEC water splitting to the improved photon absorption and facilitated charge transfer kinetics also resulting from the formation of the heterojunction structure (ibid. 2017). While different materials have been used to form the heterojunction structure with α-Fe$_2$O$_3$ for PEC applications, the choice of the composite material is important for achieving a notable improvement in water splitting efficiency. Materials that can enhance light absorption and promote

charge transport can play a significant role in boosting the photocurrent density of α-Fe_2O_3-based heterojunction photocatalysts.

3.2.4. The Use of Co-Catalysts

One of the biggest challenges of PEC water splitting using α-Fe_2O_3 is the overpotential required to drive the water oxidation reaction due to its high activation energy barrier. The presence of a co-catalyst on photoanodes can improve PEC water splitting by facilitating water oxidation reactions and decreasing the overpotential and activation energy, thus shifting the onset potential to a more negative value (Tamirat et al. 2016).

Noble metal oxides (Badia-Bou et al. 2013), amorphous phosphates (Eftekharinia et al. 2017; Kwon et al. 2021), borates (Dang et al. 2017), and oxyhydroxides (Kim et al. 2016b) have been used as co-catalysts on α-Fe_2O_3 photoanodes. α-Fe_2O_3 has been modified with the iridium oxide (IrO_2) co-catalyst and used as a photoanode in PEC water splitting, yielding a photocurrent density of 200 $\mu A/cm^2$ at 1.29 V vs. RHE, while the pristine films required a positive shift of 300 mV to achieve the same photoresponse. The IrO_2 co-catalyst promoted charge separation and acted as a storage site for photogenerated holes, leading to an improvement in PEC water splitting achieved for modified α-Fe_2O_3 films (Badia-Bou et al. 2013). Additionally, the cobalt-phosphate (Co-Pi) co-catalyst has been used to modify α-Fe_2O_3 photoanodes and recorded a photocurrent density of 1.5 mA/cm^2 at 1.5 V vs. RHE, plus a negative shift of 185 mV in the onset potential. The improved performance was also attributed to the catalytic property of Co-Pi which can capture photogenerated holes, leading to suppressed charge recombination and facilitating water oxidation (Eftekharinia et al. 2017). Elsewhere, Kim et al. (2016b) used ultra-thin amorphous FeOOH as a co-catalyst on an α-Fe_2O_3 photoanode, recording a 2-fold increase in the photocurrent density, with an onset potential drop of about 120 mV, when applied towards PEC water splitting. The improved PEC behavior was attributed to the enhanced water oxidation kinetics and passivation of the surface states of the α-Fe_2O_3 photoanode due to the modification with the FeOOH co-catalyst (ibid. 2016b).

3.2.5. Plasmonic Enhancement Effects

Plasmonic metal nanostructures offer a promising route for improving the solar energy conversion efficiency of semiconductors (Li et al. 2013). Plasmonic metals can improve the performance of photoelectrodes in PEC water splitting via three major mechanisms. First, light scattering through localized surface

plasmonic resonance (LSPR) absorption and re-emission can prolong the mean photon path in metal/semiconductor composites, resulting in an increased capture rate of incident photons. Second, hot electrons in the metal nanostructure generated through the decay of optically excited plasmons are transferred across the Schottky barrier to the nearby semiconductor, culminating in extra photoactivity. Finally, when metal/semiconductor composite nanostructures have overlapping LSPRs and energy band gaps, a large electric field enhancement occurs near the metal nanostructure's surface, leading to increased generation of electron–hole pairs in the nearby semiconductor, a concept known as the plasmonic near-field effect (Fan et al. 2016; Augustynski et al. 2016).

In efforts to improve the photocurrent density of α-Fe_2O_3 photoanodes during PEC water splitting, plasmonic metals such as Au (Archana et al. 2015; Shinde et al. 2017) and Ag (Liu et al. 2015a; Kwon et al. 2016) have been widely employed, showing great promise. Archana et al. (2015) deposited Au nanoparticles on α-Fe_2O_3 films and achieved a photocurrent enhancement that was three times higher than that of the pristine films at 0.6 V vs. Ag/AgCl. The photocurrent enhancement was attributed to a higher generation of charge carriers due to the plasmonic effects of Au nanoparticles on the α-Fe_2O_3 films (ibid. 2015). Additionally, Ag nanoparticles deposited on hydrothermally grown α-Fe_2O_3 nanowires produced a photocurrent density of about 0.18 mA/cm^2 at 1.23 vs. RHE when utilized as photoanodes in a PEC cell, representing a 10-fold enhancement relative to the value obtained for the pristine α-Fe_2O_3. The improvement was also associated with the surface plasmonic effects of Ag nanoparticles on the α-Fe_2O_3 nanowires (Kwon et al. 2016).

3.2.6. The Use of Multiple Approaches

The simultaneous use of multiple approaches to produce a single photoelectrode is a concept which harnesses the benefits of the different approaches to enhancing the PEC performance of hematite to produce a synergetic effect. The concurrent use of different approaches to produce a more efficient photocatalyst has been exploited by researchers with some significant successes recorded. Table 2 shows a list of hematite-based photoanodes in which multiple approaches to enhancing PEC performance were implemented, yielding a synergetic effect and an enhanced photocatalytic response.

Table 2. Hematite-based photoanodes in which multiple approaches to enhancing PEC performance were implemented.

Hematite-Based Photoelectrode	Strategies Engaged	Photocurrent Density Achieved Under 1 Sun	Photocurrent Density Increase Relative to That of Pristine α-Fe$_2$O$_3$	Reference
Ti-doped α-Fe$_2$O$_3$	Nanostructuring, doping	2.1 mA/cm^2 at 0.67 V vs. Ag/AgCl in 1 M NaOH electrolyte	2.8 times	(Lee et al. 2014)
α-Fe$_2$O$_3$/Co-Pi	Nanostructuring, co-catalyst loading	1.5 mA/cm^2 at 1.5 V vs. RHE 1 M NaOH electrolyte	1.39 times	(Eftekharinia et al. 2017)
α-Fe$_2$O$_3$/Au	Nanostrucring, plasmonic effects	1.0 mA/cm^2 at 1.23 V$_{RHE}$ in 1 M KOH electrolyte	2.86 times	(Wang et al. 2015)
α-Fe$_2$O$_3$/NiO	Nanostructing, heterojunction	1.55 mA/cm^2 at 1 V vs. RHE in 1M KOH electrolyte	19.37 times	(Rajendran et al. 2015)
α-Fe$_2$O$_3$/BiVO$_4$/NiFe-LDH	Nanostructuring, heterojunction, co-catalyst	1.7 mA/cm^2 at 1.8 V vs. RHE in 1 M NaOH electrolyte	4.25 times	(Bai et al. 2018)
Pt-doped α-Fe$_2$O$_3$/Co-Pi	Nanostructuring, doping, co-catalyst	4.32 mA/cm^2 at 1.23 V vs. RHE in 1 M NaOH electrolyte	3.43 times	(Kim et al. 2013)
Ti-doped α-Fe$_2$O$_3$/Cu$_2$O	Nanostructuring, doping, heterojunction	2.60 mA/cm^2 at 0.95 V vs. SCE in 1 M NaOH electrolyte	16.25 times	(Sharma et al. 2015)
α-Fe$_2$O$_3$/Au/Co-Pi	Nanostructuring, plasmonic effects, co-catalyst	4.68 mA/cm^2 at 1.23 V vs. RHE in 1 M NaOH electrolyte	3 times	(Peerakiatkhajohn et al. 2016)
α-Fe$_2$O$_3$/Nb-doped SnO$_2$/Co-Pi	Nanostructuring, heterojunction, doping, co-catalyst	3.16 mA/cm^2 at 1.23 V vs. RHE in . . . electrolyte under 1 sun	not given	(Yan et al. 2017)

Bai et al. (2018) in their work improved the performance of an α-Fe$_2$O$_3$ photoanode by combining the concepts of nanostructuring, heterojunction formation, and the use of co-catalysts. In their work, an α-Fe$_2$O$_3$/BiVO$_4$/NiFe-LDH photoanode was fabricated and applied towards PEC water splitting. A maximum photocurrent

density of 1.7 mA/cm^2 was attained by the photoanode at 1.8 V vs. RHE, representing 1.3 and 4.25 times increases compared to the values obtained for α-Fe$_2$O$_3$/BiVO$_4$ and α-Fe$_2$O$_3$ films at the same potential, respectively (ibid. 2018). Elsewhere, Kim et al. (2013) prepared doped nanostructured α-Fe$_2$O$_3$ with the Pt dopant followed by surface modification with a Co-Pi co-catalyst-based photoanode when applied towards PEC water splitting. The doping of the pristine α-Fe$_2$O$_3$ photoanode with Pt increased its photocurrent density by 74% to 2.19 mA/cm^2 at 1.23 V vs. RHE, which was further enhanced to 4.32 mA/cm^2 at the same potential after loading with the Co-Pi co-catalyst (ibid. 2013). In a similar approach, Peerakiatkhajohn et al. (2016) demonstrated the synergetic effect of coating hematite nanosheets with Au nanoparticles for a plasmonic effect, followed by loading the surface with the Co-Pi co-catalyst, and achieved a photocurrent of 4.68 mA/cm (at 1.23 V vs. RHE), which is one of the highest performances reported in the literature for a modified hematite photoanode (ibid. 2016). The improved performances obtained for hematite-based photoanodes through the use of multiple approaches were achieved by harnessing the benefits of the different methods of boosting PEC performance via the systematic application of interface engineering.

4. Conclusion

In this chapter, promising materials for solar energy harnessing have been discussed with a special focus on HaP and α-Fe$_2$O$_3$ for direct conversion into electricity and hydrogen fuels, respectively. Long-term stability is an important requirement for the sustainable transfer of HaP solar cells from the laboratory to the market. The instability of perovskite solar cells depends on the Goldschmidt tolerance, chemical composition, and defects in halide perovskites. Other components of the solar cell architecture including the back-metal contact and the charge transport layers greatly contribute to the instability of the device. All these issues are responsible for the extremely low T_{80} (less than 2 years) for perovskite solar cells as opposed to the commercially available solar cells with T_{80} lifetimes exceeding 20 years. Protecting metal top contacts from reacting with halide perovskites, passivation of 2D perovskites to form 2D/3D mixed-dimensional perovskites, encapsulation of the devices and modules, and focusing on MA-free perovskites are credible strategies that, if well developed, will enhance the long-term stability and lifetime of perovskite solar cells. The intrinsic properties of α-Fe$_2$O$_3$ films such as their poor conductivity and short carrier lifetime have continued to limit their application for solar hydrogen production. Various strategies for improving the durability of HaP solar cells and the efficiency of α-Fe$_2$O$_3$ films in photocatalytic

hydrogen production were discussed. The use of additives to achieve large grain sizes with few grain boundaries and to passivate the surface and boundaries of HaP is effective in improving the stability of HaP solar cells. Meanwhile, the concurrent use of multiple approaches such as nanostructuring, doping, the formation of heterostructures, the use of co-catalysts, and plasmonic enhancement effects has shown great promise in improving the photocatalytic efficiency of α-Fe$_2$O$_3$-based films for solar hydrogen production. Further research is still required for the eventual commercialization of solar hydrogen production and photovoltaic technologies using α-Fe$_2$O$_3$ and HaP, respectively.

Author Contributions: Conceptualization, J.N.F., and P.I.K.; methodology, J.N.F., and P.I.K.; software, J.N.F., and P.I.K.; validation, J.N.F., P.I.K., and M.D.; formal analysis, J.N.F., and P.I.K.; investigation, J.N.F., and P.I.K.; resources, J.N.F., P.I.K., and M.D.; data curation, J.N.F., and P.I.K.; writing—original draft preparation, J.N.F., and P.I.K.; writing—review and editing, J.N.F., and P.I.K.; visualization, J.N.F., and P.I.K.; supervision, M.D.; project administration, J.N.F., and P.I.K.; funding acquisition, M.D. substantially to the work reported.

Conflicts of Interest: The authors declare no conflict of interest.

References

Abdi-jalebi, Mojtaba, Zahra Andaji-garmaroudi, Stefania Cacovich, Camille Stavrakas, Bertrand Philippe, Eline M. Hutter, Andrew J. Pearson, Samuele Lilliu, Tom J. Savenije, Håkan Rensmo, and et al. 2018. Halide Perovskites with Potassium Passivation. *Nature Publishing Group* 555: 497–501. [CrossRef]

Afroz, Khurshida, Md Moniruddin, Nurlan Bakranov, Sarkyt Kudaibergenov, and Nurxat Nuraje. 2018. A Heterojunction Strategy to Improve the Visible Light Sensitive Water Splitting Performance of Photocatalytic Materials. *Journal of Materials Chemistry A* 6: 21696–718. [CrossRef]

Ahn, Hyo Jin, Myung Jun Kwak, Jung Soo Lee, Ki Yong Yoon, and Ji Hyun Jang. 2014. Nanoporous Hematite Structures to Overcome Short Diffusion Lengths in Water Splitting. *Journal of Materials Chemistry A* 2: 19999–20003. [CrossRef]

Annamalai, Alagappan, Pravin S. Shinde, Tae Hwa Jeon, Hyun Hwi Lee, Hyun Gyu Kim, Wonyong Choi, and Jum Suk Jang. 2016. Fabrication of Superior α-Fe$_2$O$_3$ Nanorod Photoanodes through Ex-Situ Sn-Doping for Solar Water Splitting. *Solar Energy Materials and Solar Cells* 144: 247–55. [CrossRef]

Aranda, Clara A., Laura Caliò, and Manuel Salado. 2021. Toward Commercialization of Stable Devices: An Overview on Encapsulation of Hybrid Organic-Inorganic Perovskite Solar Cells. *Crystals* 11: 1–16. [CrossRef]

Archana, Panikar Sathyaseelan, Neha Pachauri, Zhichao Shan, Shanlin Pan, and Arunava Gupta. 2015. Plasmonic Enhancement of Photoactivity by Gold Nanoparticles Embedded in Hematite Films. *Journal of Physical Chemistry C* 119: 15506–16. [CrossRef]

Augustynski, Jan, Krzysztof Bienkowski, and Renata Solarska. 2016. Plasmon Resonance-Enhanced Photoelectrodes and Photocatalysts. *Coordination Chemistry Reviews* 325: 116–24. [CrossRef]

Babu, Vivek, Rosinda Fuentes Pineda, Taimoor Ahmad, Agustin O. Alvarez, Luigi Angelo Castriotta, Aldo Di Carlo, Francisco Fabregat-Santiago, and Konrad Wojciechowski. 2020. Improved Stability of Inverted and Flexible Perovskite Solar Cells with Carbon Electrode. *ACS Applied Energy Materials* 3: 5126–34. [CrossRef]

Back, Hyungcheol, Geunjin Kim, Junghwan Kim, Jaemin Kong, Tae Kyun Kim, Hongkyu Kang, Heejoo Kim, Jinho Lee, Seongyu Lee, and Kwanghee Lee. 2016. Achieving Long-Term Stable Perovskite Solar Cells: Via Ion Neutralization. *Energy and Environmental Science* 9: 1258–63. [CrossRef]

Badia-Bou, Laura, Elena Mas-Marza, Pau Rodenas, Eva M. Barea, Francisco Fabregat-Santiago, Sixto Gimenez, Eduardo Peris, and Juan Bisquert. 2013. Water Oxidation at Hematite Photoelectrodes with an Iridium-Based Catalyst. *Journal of Physical Chemistry C* 117: 3826–33. [CrossRef]

Bai, Shouli, Haomiao Chu, Xu Xiang, Ruixian Luo, Jing He, and Aifan Chen. 2018. Fabricating of Fe$_2$O$_3$/BiVO$_4$ Heterojunction Based Photoanode Modified with NiFe-LDH Nanosheets for Efficient Solar Water Splitting. *Chemical Engineering Journal* 350: 148–56. [CrossRef]

Bemana, Hossein, and Sahar Rashid-Nadimi. 2017. Effect of Sulfur Doping on Photoelectrochemical Performance of Hematite. *Electrochimica Acta* 229: 396–403. [CrossRef]

Bemana, Hossein, and Sahar Rashid-Nadimi. 2019. Incorporation of NiO Electrocatalyst with α-Fe$_2$O$_3$ Photocatalyst for Enhanced and Stable Photoelectrochemical Water Splitting. *Surfaces and Interfaces* 14: 184–91. [CrossRef]

Benato, Alberto, and Anna Stoppato. 2018. Pumped Thermal Electricity Storage: A Technology Overview. *Thermal Science and Engineering Progress* 6: 301–15. [CrossRef]

Boyd, Caleb C., Rongrong Cheacharoen, Kevin A. Bush, Rohit Prasanna, Tomas Leijtens, and Michael D. McGehee. 2018. Barrier Design to Prevent Metal-Induced Degradation and Improve Thermal Stability in Perovskite Solar Cells. *ACS Energy Letters* 3: 1772–78. [CrossRef]

Bush, Kevin A., Axel F. Palmstrom, Zhengshan J. Yu, Mathieu Boccard, Rongrong Cheacharoen, Jonathan P. Mailoa, David P. McMeekin, Robert L. Z. Hoye, Colin D. Bailie, Tomas Leijtens, and et al. 2017. 23.6%-Efficient Monolithic Perovskite/Silicon Tandem Solar Cells With Improved Stability. *Nature Energy* 2: 1–7. [CrossRef]

Cao, Duyen H., Constantinos C. Stoumpos, Omar K. Farha, Joseph T. Hupp, and Kanatzidis G. Mercouri. 2015. 2D Homologous Perovskites as Light-Absorbing Materials for Solar Cell Applications. *Journal of the American Chemical Society* 137: 7843–50. [CrossRef]

Cattarin, Sandro, and Franco Decker. 2009. Electrodes | Semiconductor Electrodes. *Encyclopedia of Electrochemical Power Sources* 9: 121–33. [CrossRef]

Cheacharoen, Rongrong, Nicholas Rolston, Duncan Harwood, Kevin A. Bush, Reinhold H. Dauskardt, and Michael D. McGehee. 2018. Design and Understanding of Encapsulated Perovskite Solar Cells to Withstand Temperature Cycling. *Energy and Environmental Science* 11: 144–50. [CrossRef]

Chen, Haoran, Yuetian Chen, Taiyang Zhang, Xiaomin Liu, Xingtao Wang, and Yixin Zhao. 2021. Advances to High-Performance Black-Phase FAPbI$_3$ Perovskite for Efficient and Stable Photovoltaics. *Small Structures* 2: 2000130. [CrossRef]

Chen, Peng, Yang Bai, Songcan Wang, Miaoqiang Lyu, Jung-ho Yun, and Lianzhou Wang. 2018. In Situ Growth of 2D Perovskite Capping Layer for Stable and Efficient Perovskite Solar Cells. *Advanced Functional Materials* 28: 1706923. [CrossRef]

Chen, Qi, Huanping Zhou, Tze-bin Song, Song Luo, Ziruo Hong, Hsin-sheng Duan, Letian Dou, Yongsheng Liu, and Yang Yang. 2014. Controllable Self-Induced Passivation of Hybrid Lead Iodide Perovskites toward High-Performance Solar Cells. *Nano Letters* 14: 4158–63. [CrossRef] [PubMed]

Chou, Jen Chun, Szu An Lin, Chi Young Lee, and Jon Yiew Gan. 2013. Effect of Bulk Doping and Surface-Trapped States on Water Splitting with Hematite Photoanodes. *Journal of Materials Chemistry A* 1: 5908–14. [CrossRef]

Dang, Ke, Tuo Wang, Chengcheng Li, Jijie Zhang, Shanshan Liu, and Jinlong Gong. 2017. Improved Oxygen Evolution Kinetics and Surface States Passivation of Ni-Bi Co-Catalyst for a Hematite Photoanode. *Engineering* 3: 285–89. [CrossRef]

DeQuilettes, Dane W., Sarah M. Vorpahl, Samuel D. Stranks, Hirokazu Nagaoka, Giles E. Eperon, Mark E. Ziffer, Henry J. Snaith, and David S. Ginger. 2015. Impact of Microstructure on Local Carrier Lifetime in Perovskite Solar Cells. *Science* 348: 683–86. [CrossRef]

Dewinggih, Tanti, Shobih, Lia Muliani, Herman, and Rahmat Hidayat. 2017. The Temperature Effect on the Working Characteristics of Solar Cells Based on Organometal Halide Perovskite Crystals The Temperature Effect on the Working Characteristics of Solar Cells Based on Organometal Halide Perovskite Crystals. *Journal of Physics: Conference Series* 877: 012043. [CrossRef]

Dias, Paula, Tânia Lopes, Luísa Andrade, and Adélio Mendes. 2014. Temperature Effect on Water Splitting Using a Si-Doped Hematite Photoanode. *Journal of Power Sources* 272: 567–80. [CrossRef]

Domanski, Konrad, Juan Pablo Correa-Baena, Nicolas Mine, Mohammad Khaja Nazeeruddin, Antonio Abate, Michael Saliba, Wolfgang Tress, Anders Hagfeldt, and Michael Grätzel. 2016. Not All That Glitters Is Gold: Metal-Migration-Induced Degradation in Perovskite Solar Cells. *ACS Nano* 10: 6306–14. [CrossRef]

Dunn, Bruce, Yang Yang, Mingkui Wang, Lijian Zuo, Hexia Guo, Nicholas De Marco, David S. Ginger, Bruce Dunn, Mingkui Wang, and Yang Yang. 2017. Polymer-Modified Halide Perovskite Films for Efficient and Stable Planar Heterojunction Solar Cells. *Science Advances* 3: e1700106. [CrossRef]

Eftekhari, Ali, Veluru Jagadeesh Babu, and Seeram Ramakrishna. 2017. Photoelectrode Nanomaterials for Photoelectrochemical Water Splitting. *International Journal of Hydrogen Energy* 42: 11078–109. [CrossRef]

Eftekharinia, Behrooz, Ahmad Moshaii, Ali Dabirian, and Nader Sobhkhiz Vayghan. 2017. Optimization of Charge Transport in a Co-Pi Modified Hematite Thin Film Produced by Scalable Electron Beam Evaporation for Photoelectrochemical Water Oxidation. *Journal of Materials Chemistry A* 5: 3412–24. [CrossRef]

Eidsvåg, Håkon, Said Bentouba, Ponniah Vajeeston, Shivatharsiny Yohi, and Dhayalan Velauthapillai. 2021. TiO_2 as a Photocatalyst for Water Splitting—An Experimental and Theoretical Review. *Molecules* 26: 1–30. [CrossRef] [PubMed]

Emami, Seyedali, Jorge Martins, Dzmitry Ivanou, and Adélio Mendes. 2020. Advanced Hermetic Encapsulation of Perovskite Solar Cells: The Route to Commercialization. *Journal of Materials Chemistry A* 8: 2654–62. [CrossRef]

Fan, Wenguang, Michael K. H. Leung, Jimmy C. Yu, and Wing Kei Ho. 2016. Recent Development of Plasmonic Resonance-Based Photocatalysis and Photovoltaics for Solar Utilization. *Molecules* 21: 180. [CrossRef]

Fang, Zhibin, Wenjing Chen, Yongliang Shi, Jin Zhao, Shenglong Chu, and Ji Zhang. 2020. Dual Passivation of Perovskite Defects for Light-Emitting Diodes with External Quantum Efficiency Exceeding 20%. *Advanced Functional Materials* 30: 1909754. [CrossRef]

Fantanas, Dimitrios, Adam Brunton, Simon J. Henley, and Robert A. Dorey. 2018. Investigation of the mechanism for current induced network failure for spray deposited silver nanowires. *Nanotechnology* 29: 465705. [CrossRef]

Feng, Fan, Can Li, Jie Jian, Fan Li, Youxun Xu, Hongqiang Wang, and Lichao Jia. 2020. Gradient Ti-Doping in Hematite Photoanodes for Enhanced Photoelectrochemical Performance. *Journal of Power Sources* 449: 227473. [CrossRef]

Fru, Juvet N., Nolwazi Nombona, and Mmantsae Diale. 2021. Growth and Degradation of Methylammonium Lead Tri-Bromide Perovskite Thin Film at Metal/Perovskite Interfaces. *Thin Solid Films* 722: 138568. [CrossRef]

Glanz, Karen. 2010. Using Behavioral Theories to Guide Decisions of What to Measure, and Why. *International Journal of Hydrogen Energy* 27: 991–1022.

Grancini, Giulia, Cristina Roldán-Carmona, Ivan Zimmermann, Edoardo Mosconi, Xuhui Lee, Daniel Martineau, Stéphanie Narbey, F. Oswald, F. De Angelis, M. Graetzel, and et al. 2017. One-Year Stable Perovskite Solar Cells by 2D/3D Interface Engineering. *Nature Communications* 8: 1–8. [CrossRef]

Grave, Daniel A., Natav Yatom, David S. Ellis, Maytal Caspary Toroker, and Avner Rothschild. 2018. The 'Rust' Challenge: On the Correlations between Electronic Structure, Excited State Dynamics, and Photoelectrochemical Performance of Hematite Photoanodes for Solar Water Splitting. *Advanced Materials* 30: 1–10. [CrossRef] [PubMed]

Griffini, Gianmarco, and Stefano Turri. 2016. Polymeric Materials for Long-Term Durability of Photovoltaic Systems. *Journal of Applied Polymer Science* 133: 1–16. [CrossRef]

Grigorescu, Sabina, Chong-yong Lee, Kiyoung Lee, Sergiu Albu, Indhumati Paramasivam, Ioana Demetrescu, and Patrik Schmuki. 2012. Electrochemistry Communications Thermal Air Oxidation of Fe: Rapid Hematite Nanowire Growth and Photoelectrochemical Water Splitting Performance. *Electrochemistry Communications* 23: 59–62. [CrossRef]

Gurudayal, Sing Yang Chiam, Mulmudi Hemant Kumar, Prince Saurabh Bassi, Hwee Leng Seng, James Barber, and Lydia Helena Wong. 2014. Improving the Efficiency of Hematite Nanorods for Photoelectrochemical Water Splitting by Doping with Manganese. *ACS Applied Materials and Interfaces* 6: 5852–59. [CrossRef] [PubMed]

Han, Yu, Steffen Meyer, Yasmina Dkhissi, Karl Weber, Jennifer M. Pringle, Udo Bach, Leone Spiccia, and Yi-Bing Cheng. 2015. Degradation Observations of Encapsulated Planar $CH_3NH_3PbI_3$ Perovskite Solar Cells at High Temperatures and Humidity. *Journal of Materials Chemistry A* 3: 8139–47. [CrossRef]

He, Sisi, Longbin Qiu, Luis K. Ono, and Yabing Qi. 2020. How Far Are We from Attaining 10-Year Lifetime for Metal Halide Perovskite Solar Cells? *Materials Science and Engineering R: Reports* 140: 100545. [CrossRef]

Hoke, Eric T., Daniel J. Slotcavage, Emma R. Dohner, Andrea R. Bowring, Hemamala I. Karunadasa, and Michael D. McGehee. 2015. Reversible Photo-Induced Trap Formation in Mixed-Halide Hybrid Perovskites for Photovoltaics. *Chemical Science* 6: 613–17. [CrossRef]

Fujishima, Akira, and Kenichi Honda. 1972. Electrochemical Photolysis of Water at a Semiconductor Electrode. *Nature* 238: 737–40. [CrossRef]

Hsieh, Cheng-ming, Yung-sheng Liao, Yan-ru Lin, Chih-ping Chen, Cheng-min Tsai, Eric Wei-guang Diau, and Shih-ching Chuang. 2018. Of Perovskite Solar Cells Using Lewis Bases Urea and Thiourea as Additives: Stimulating Large Grain. *RSC Advances* 8: 19610–15. [CrossRef]

Idígoras, Jesús, Francisco J. Aparicio, Lidia Contreras-Bernal, Susana Ramos-Terrón, María Alcaire, Juan Ramón Sánchez-Valencia, Ana Borras, Ángel Barranco, and Juan A. Anta. 2018. Enhancing Moisture and Water Resistance in Perovskite Solar Cells by Encapsulation with Ultrathin Plasma Polymers. *ACS Applied Materials and Interfaces* 10: 11587–94. [CrossRef]

Ierides, Ioannis, Isaac Squires, Giulia Lucarelli, Thomas M. Brown, and Franco Cacialli. 2021. Inverted Organic Photovoltaics with a Solution-Processed ZnO/MgO Electron Transport Bilayer. *Journal of Materials Chemistry C* 9: 3901–10. [CrossRef]

Ihssen, Julian, Artur Braun, Greta Faccio, Krisztina Gajda-Schrantz, and Linda Thöny-Meyer. 2014. Light Harvesting Proteins for Solar Fuel Generation in Bioengineered Photoelectrochemical Cells. *Current Protein & Peptide Science* 15: 374–84. [CrossRef]

Ito, Nathalie Minko, Waldemir Moura Carvalho, Dereck Nills Ferreira Muche, Ricardo Hauch Ribeiro Castro, Gustavo Martini Dalpian, and Flavio Leandro Souza. 2017. High Temperature Activation of Hematite Nanorods for Sunlight Driven Water Oxidation Reaction. *Physical Chemistry Chemical Physics* 19: 25025–32. [CrossRef] [PubMed]

Jain, Deepak, Suryanaman Chaube, Prerna Khullar, Sriram Goverapet Srinivasan, and Beena Rai. 2019. Bulk and Surface DFT Investigations of Inorganic Halide Perovskites Screened Using Machine Learning and Materials Property Databases. *Physical Chemistry Chemical Physics* 21: 19423–36. [CrossRef] [PubMed]

Jeong, Jaeki, Minjin Kim, Jongdeuk Seo, Haizhou Lu, Paramvir Ahlawat, Aditya Mishra, Yingguo Yang, Michael A. Hope, Felix T. Eickemeyer, Maengsuk Kim, and et al. 2021. Pseudo-Halide Anion Engineering for α-FAPbI$_3$ Perovskite Solar Cells. *Nature* 592: 381–85. [CrossRef]

Jiang, Qi, Yang Zhao, Xingwang Zhang, Xiaolei Yang, Yong Chen, Zema Chu, Qiufeng Ye, Xingxing Li, Zhigang Yin, and Jingbi You. 2019. Surface Passivation of Perovskite Film for Efficient Solar Cells. *Nature Photonics* 13: 460–66. [CrossRef]

Jin, Handong, Elke Debroye, Masoumeh Keshavarz, Ivan G. Scheblykin, Maarten B. J. Roeffaers, and Julian A. Steele. 2020. It's a Trap ! On the Nature of Localised States and Charge Trapping in Lead Halide Perovskites. *Materials Horizons* 7: 397–410. [CrossRef]

Juarez-Perez, Emilio J., Luis K. Ono, Maki Maeda, Yan Jiang, Zafer Hawash, and Yabing Qi. 2018. Photodecomposition and Thermal Decomposition in Methylammonium Halide Lead Perovskites and Inferred Design Principles to Increase Photovoltaic Device Stability. *Journal of Materials Chemistry A* 6: 9604–12. [CrossRef]

Juarez-Perez, Emilio J., Luis K. Ono, and Yabing Qi. 2019. Thermal Degradation of Formamidinium Based Lead Halide Perovskites into *Sym*-Triazine and Hydrogen Cyanide Observed by Coupled Thermogravimetry-Mass Spectrometry Analysis. *Journal of Materials Chemistry A* 7: 16912–19. [CrossRef]

Kafizas, Andreas, Robert Godin, and James R. Durrant. 2017. Charge Carrier Dynamics in Metal Oxide Photoelectrodes for Water Oxidation. *Semiconductors and Semimetals* 97: 3–46. [CrossRef]

Kaltenbrunner, Martin, Getachew Adam, Eric Daniel Głowacki, Michael Drack, Reinhard Schwödiauer, Lucia Leonat, Dogukan Hazar Apaydin, Heiko Groiss, Markus Clark Scharber, Matthew Schuette White, and et al. 2015. Flexible High Power-per-Weight Perovskite Solar Cells with Chromium Oxide-Metal Contacts for Improved Stability in Air. *Nature Materials* 14: 1032–39. [CrossRef] [PubMed]

Kang, Keehoon, Heebeom Ahn, Younggul Song, Woocheol Lee, Junwoo Kim, Youngrok Kim, Daekyoung Yoo, and Takhee Lee. 2019. High-Performance Solution-Processed Organo-Metal Halide Perovskite Unipolar Resistive Memory Devices in a Cross-Bar Array Structure. *Advanced Materials* 31: 1804841. [CrossRef] [PubMed]

Kim, Do Hong, Dinsefa M. Andoshe, Young Seok Shim, Cheon Woo Moon, Woonbae Sohn, Seokhoon Choi, Taemin Ludvic Kim, Migyoung Lee, Hoonkee Park, Kootak Hong, and et al. 2016a. Toward High-Performance Hematite Nanotube Photoanodes: Charge-Transfer Engineering at Heterointerfaces. *ACS Applied Materials and Interfaces* 8: 23793–800. [CrossRef] [PubMed]

Kim, Jae Young, Duck Hyun Youn, Kyoungwoong Kang, and Jae Sung Lee. 2016b. Highly Conformal Deposition of an Ultrathin FeOOH Layer on a Hematite Nanostructure for Efficient Solar Water Splitting. *Angewandte Chemie - International Edition* 55: 10854–58. [CrossRef] [PubMed]

Kim, Gee Yeong, Alessandro Senocrate, Tae Youl Yang, Giuliano Gregori, Michael Grätzel, and Joachim Maier. 2018. Large Tunable Photoeffect on Ion Conduction in Halide Perovskites and Implications for Photodecomposition. *Nature Materials* 17: 445–49. [CrossRef]

Kim, Jae Young, Ganesan Magesh, Duck Hyun Youn, Ji Wook Jang, Jun Kubota, Kazunari Domen, and Jae Sung Lee. 2013. Single-Crystalline, Wormlike Hematite Photoanodes for Efficient Solar Water Splitting. *Scientific Reports* 3: 1–8. [CrossRef]

Kim, Jongseob, Sung-hoon Lee, Jung Hoon Lee, and Ki-ha Hong. 2014. The Role of Intrinsic Defects in Methylammonium Lead Iodide. *The journal of physical chemistry letters* 5: 1312–17. [CrossRef]

Kong, Weiguang, Tao Ding, Gang Bi, and Huizhen Wu. 2016. Optical Characterizations of the Surface States in Hybrid Lead–Halide Perovskites. *Physical Chemistry Chemical Physics* 18: 12626–32. [CrossRef]

Kwon, In, Mahadeo A. Mahadik, Jun Beom, Weon-sik Chae, Sun Hee, and Jum Suk. 2021. Lowering the Onset Potential of Zr-Doped Hematite Nanocoral Photoanodes by Al Co-Doping and Surface Modification with Electrodeposited Co–Pi. *Journal of Colloid And Interface Science* 581: 751–63. [CrossRef]

Kwon, Jinhyeong, Junyeob Yeo, Sukjoon Hong, Young D. Suh, Habeom Lee, Jun Ho Choi, Seung S. Lee, and Seung Hwan Ko. 2016. Photoreduction Synthesis of Hierarchical Hematite/Silver Nanostructures for Photoelectrochemical Water Splitting. *Energy Technology* 4: 271–77. [CrossRef]

Kyesmen, Pannan I., Nolwazi Nombona, and Mmantsae Diale. 2021. Heterojunction of Nanostructured α-Fe$_2$O$_3$/CuO for Enhancement of Photoelectrochemical Water Splitting. *Journal of Alloys and Compounds* 863: 158724. [CrossRef]

Lee, Jin-wook, Hui-seon Kim, and Nam-gyu Park. 2015. Lewis Acid − Base Adduct Approach for High Efficiency Perovskite Solar Cells. *Accounts of chemical research* 49: 311–19. [CrossRef] [PubMed]

Lee, Myeong Hwan, Jong Hoon Park, Hyun Soo Han, Hee Jo Song, In Sun Cho, Jun Hong Noh, and Kug Sun Hong. 2014. Nanostructured Ti-Doped Hematite (α-Fe$_2$O$_3$) Photoanodes for Efficient Photoelectrochemical Water Oxidation. *International Journal of Hydrogen Energy* 39: 17501–7. [CrossRef]

Lee, Young Il, Nam Joong Jeon, Bong Jun Kim, Hyunjeong Shim, Tae Youl Yang, Sang Il Seok, Jangwon Seo, and Sung Gap Im. 2018. A Low-Temperature Thin-Film Encapsulation for Enhanced Stability of a Highly Efficient Perovskite Solar Cell. *Advanced Energy Materials* 8: 1–8. [CrossRef]

Li, Jiangtian, Scott K. Cushing, Peng Zheng, Fanke Meng, Deryn Chu, and Nianqiang Wu. 2013. Plasmon-Induced Photonic and Energy-Transfer Enhancement of Solar Water Splitting by a Hematite Nanorod Array. *Nature Communications* 4: 1–8. [CrossRef]

Li, Jinkai, Yongcai Qiu, Zhanhua Wei, Qingfeng Lin, Qianpeng Zhang, Keyou Yan, Haining Chen, Shuang Xiao, Zhiyong Fan, and Shihe Yang. 2014. A Three-Dimensional Hexagonal Fluorine-Doped Tin Oxide Nanocone Array: A Superior Light Harvesting Electrode for High Performance Photoelectrochemical Water Splitting. *Energy and Environmental Science* 7: 3651–58. [CrossRef]

Li, Mingyang, Yi Yang, Yichuan Ling, Weitao Qiu, Fuxin Wang, Tianyu Liu, Yu Song, Xiaoxia Liu, Pingping Fang, Yexiang Tong, and et al. 2017. Morphology and Doping Engineering of Sn-Doped Hematite Nanowire Photoanodes. *Nano Letters* 17: 2490–95. [CrossRef]

Li, Bixin, Wei Hui, Xueqin Ran, Yingdong Xia, Fei Xia, Lingfeng Chao, Yonghua Chen, and Wei Huang. 2019. Memory Devices and Artificial Synapses. *Journal of Materials Chemistry C* 7: 7476–93. [CrossRef]

Lin, Xiongfeng, Askhat N. Jumabekov, Niraj N. Lal, Alexander R. Pascoe, Daniel E. Gómez, Noel W. Duffy, Anthony S.R. Chesman, Kallista Sears, Maxime Fournier, Yupeng Zhang, and et al. 2017. Dipole-Field-Assisted Charge Extraction in Metal-Perovskite-Metal Back-Contact Solar Cells. *Nature Communications* 8: 1–8. [CrossRef]

Liu, Cong, Zengqi Huang, Xiaotian Hu, Xiangchuan Meng, Liqiang Huang, and Jian Xiong. 2018. Grain Boundary Modi Fi Cation via F4TCNQ To Reduce Defects of Perovskite Solar Cells with Excellent Device Performance. *ACS Applied Materials & Interfaces* 10: 1909–16. [CrossRef]

Liu, Dong, David M. Bierman, Andrej Lenert, Hai-Tong Yu, Zhen Yang, Evelyn N. Wang, and Yuan-Yuan Duan. 2015a. Ultrathin Planar Hematite Film for Solar Photoelectrochemical Water Splitting. *Optics Express* 23: A1491. [CrossRef] [PubMed]

Liu, Xiangye, Wei Zhao, Houlei Cui, Yi Xie, Yaoming Wang, Tao Xu, and Fuqiang Huang. 2015b. Organic–Inorganic Halide Perovskite Based Solar Cells–Revolutionary Progress in Photovoltaics. *Inorganic Chemistry Frontiers* 2: 584–84. [CrossRef]

Grundmann, Marius. 2010. *Physics of Semiconductors*. Berlin: Springer, vol. 11, pp. 401–72. [CrossRef]

Mansour Rezaei Fumani, Nasibeh, Farzaneh Arabpour Roghabadi, Maryam Alidaei, Seyed Mojtaba Sadrameli, Vahid Ahmadi, and Farhood Najafi. 2020. Prolonged Lifetime of Perovskite Solar Cells Using a Moisture-Blocked and Temperature-Controlled Encapsulation System Comprising a Phase Change Material as a Cooling Agent. *ACS Omega* 5: 7106–14. [CrossRef] [PubMed]

Mao, Aiming, Nam Gyu Park, Gui Young Han, and Jong Hyeok Park. 2011. Controlled Growth of Vertically Oriented Hematite/Pt Composite Nanorod Arrays: Use for Photoelectrochemical Water Splitting. *Nanotechnology* 22: 175703. [CrossRef]

Mayer, Matthew T., Chun Du, and Dunwei Wang. 2012. Hematite/Si Nanowire Dual-Absorber System for Photoelectrochemical Water Splitting at Low Applied Potentials. *Journal of the American Chemical Society* 134: 12406–9. [CrossRef]

Mckenna, Keith P. 2018. Electronic Properties of {111} Twin Boundaries in a Mixed-Ion Lead Halide Perovskite Solar Absorber. *ACS Energy Letters* 3: 2663–68. [CrossRef]

Ming, Wenmei, Dongwen Yang, Tianshu Li, Lijun Zhang, and Mao Hua Du. 2018. Formation and Diffusion of Metal Impurities in Perovskite Solar Cell Material $CH_3NH_3PbI_3$: Implications on Solar Cell Degradation and Choice of Electrode. *Advanced Science* 5: 1700662. [CrossRef]

Motti, Silvia G., Daniele Meggiolaro, Samuele Martani, Roberto Sorrentino, Alex J. Barker, Filippo De Angelis, and Annamaria Petrozza. 2019. Defect Activity in Lead Halide Perovskites. *Advanced Materials* 31: 1901183. [CrossRef]

Murphy, Anthony B., Piers R. F. Barnes, Lakshman K. Randeniya, Ian C. Plumb, Ian E. Grey, Mike D. Horne, and Julie A. Glasscock. 2006. Efficiency of Solar Water Splitting Using Semiconductor Electrodes. *International Journal of Hydrogen Energy* 31: 1999–2017. [CrossRef]

Natarajan, Kaushik, Mohit Saraf, and Shaikh M. Mobin. 2017. Visible-Light-Induced Water Splitting Based on a Novel α-Fe$_2$O$_3$/CdS Heterostructure. *ACS Omega* 2: 3447–56. [CrossRef]

Niu, Tianqi, Jing Lu, Xuguang Jia, Zhuo Xu, Ming-chun Tang, Dounya Barrit, Ningyi Yuan, Jianning Ding, Xu Zhang, Yuanyuan Fan, and et al. 2019. Interfacial Engineering at the 2D/3D Heterojunction for High-Performance Perovskite Solar Cells. *Nano Letters* 19: 7181–90. [CrossRef] [PubMed]

Noel, Nakita Kimberly, Antonio Abate, Samuel David Stranks, Elizabeth Parrott, Victor Burlakov, Alain Goriely, and Henry J. Snaith. 2014. Enhanced Photoluminescence and Solar Cell Performance via Lewis Base Passivation of Organic-Inorganic Lead Halide Perovskites. *ACS nano* 8: 9815–21. [CrossRef] [PubMed]

Rothmann, Mathias Uller, Wei Li, Ye Zhu, Udo Bach, Leone Spiccia, Joanne Etheridge, and Yi-Bing Cheng. 2017. Direct observation of intrinsic twin domains in tetragonal CH$_3$NH$_3$PbI$_3$. *Nature Communications* 8: 6–13. [CrossRef] [PubMed]

Peerakiatkhajohn, Piangjai, Jung Ho Yun, Hongjun Chen, Miaoqiang Lyu, Teera Butburee, and Lianzhou Wang. 2016. Stable Hematite Nanosheet Photoanodes for Enhanced Photoelectrochemical Water Splitting. *Advanced Materials* 28: 6405–10. [CrossRef] [PubMed]

Peng, Yong, Qingdong Ruan, Chun Ho Lam, Fanxu Meng, Chung-yu Guan, Shella Permatasari Santoso, Xingli Zou, Edward T. Yu, Paul K. Chu, and Hsien-yi Hsu. 2021. Plasma-Implanted Ti-Doped Hematite Photoanodes with Enhanced Photoelectrochemical Water Oxidation Performance. *Journal of Alloys and Compounds* 870: 159376. [CrossRef]

Qiao, Lu, Wei-hai Fang, and Run Long. 2019. Forschungsartikel Extending Carrier Lifetimes in Lead Halide Perovskites with Alkali Metals by Passivating and Eliminating Halide Interstitial Defects Forschungsartikel. *Angewandte Chemie* 132: 4714–20. [CrossRef]

Qiu, Longbin, Sisi He, Luis K. Ono, and Yabing Qi. 2020. Progress of Surface Science Studies on ABX$_3$-Based Metal Halide Perovskite Solar Cells. *Advanced Energy Materials* 10: 1902726. [CrossRef]

Rahmany, Stav, and Lioz Etgar. 2021. Two-Dimensional or Passivation Treatment: The Effect of Hexylammonium Post Deposition Treatment on 3D Halide Perovskite-Based Solar Cells. *Materials Advances* 2: 2617–25. [CrossRef]

Rajendran, Kumar, Vithiya Karunagaran, Biswanath Mahanty, and Shampa Sen. 2015. Biosynthesis of Hematite Nanoparticles and Its Cytotoxic Effect on HepG2 Cancer Cells. *International Journal of Biological Macromolecules* 74: 376–81. [CrossRef]

Rani, Ankita, Rajesh Reddy, Uttkarshni Sharma, Priya Mukherjee, Priyanka Mishra, Aneek Kuila, Lan Ching Sim, and Pichiah Saravanan. 2018. A Review on the Progress of Nanostructure Materials for Energy Harnessing and Environmental Remediation. *Journal of Nanostructure in Chemistry* 8: 255–91. [CrossRef]

Ruddlesden, S. N., and Paul Popper. 1958. The Compound $Sr_3Ti_2O_7$ and Its Structure. *Acta Crystallographica* 11: 54–55. [CrossRef]

Sanehira, Erin M., Bertrand J. Tremolet De Villers, Philip Schulz, Matthew O. Reese, Suzanne Ferrere, Kai Zhu, Lih Y. Lin, Joseph J. Berry, and Joseph M. Luther. 2016. Influence of Electrode Interfaces on the Stability of Perovskite Solar Cells: Reduced Degradation Using MoO_x/Al for Hole Collection. *ACS Energy Letters* 1: 38–45. [CrossRef]

Selim, Shababa, Laia Francàs, Miguel García-Tecedor, Sacha Corby, Chris Blackman, Sixto Gimenez, James R. Durrant, and Andreas Kafizas. 2019. WO_3/$BiVO_4$: Impact of Charge Separation at the Timescale of Water Oxidation. *Chemical Science* 10: 2643–52. [CrossRef]

Asad, Jihad, Samy K. K. Shaat, Hussam Musleh, Nabil Shurrab, Ahmed Issa, Abelilah Lahmar, Amal Al-Kahlout, and Naji Al Dahoudi. 2019. Perovskite Solar Cells Free of Hole Transport Layer. *Journal of Sol-Gel Science and Technology*, 443–49. [CrossRef]

Shao, Yuchuan, Yanjun Fang, Tao Li, Qi Wang, Qingfeng Dong, Yehao Deng, Yongbo Yuan, Haotong Wei, Meiyu Wang, Alexei Gruverman, and et al. 2016. Environmental Science Grain Boundary Dominated Ion Migration in Polycrystalline Organic – Inorganic Halide Perovskite Films. *Energy & Environmental Science* 9: 1752–59. [CrossRef]

Shao, Yuchuan, Zhengguo Xiao, Cheng Bi, Yongbo Yuan, and Jinsong Huang. 2014. Origin and Elimination of Photocurrent Hysteresis by Fullerene Passivation in $CH_3NH_3PbI_3$ Planar Heterojunction Solar Cells. *Nature Communications* 5: 1–7. [CrossRef] [PubMed]

Sharma, Dipika, Sumant Upadhyay, Anuradha Verma, Vibha R. Satsangi, Rohit Shrivastav, and Sahab Dass. 2015. Nanostructured Ti-Fe_2O_3/Cu_2O Heterojunction Photoelectrode for Efficient Hydrogen Production. *Thin Solid Films* 574: 125–31. [CrossRef]

Shen, Shaohua, Jigang Zhou, Chung Li Dong, Yongfeng Hu, Eric Nestor Tseng, Penghui Guo, Liejin Guo, and Samuel S. Mao. 2014. Surface Engineered Doping of Hematite Nanorod Arrays for Improved Photoelectrochemical Water Splitting. *Scientific Reports* 4: 1–9. [CrossRef]

Sherkar, Tejas S., Cristina Momblona, A. Jorge, Michele Sessolo, Henk J. Bolink, and L. Jan Anton Koster. 2017. Recombination in Perovskite Solar Cells: Significance of Grain Boundaries, Interface Traps, and Defect Ions. *ACS Energy Letters* 2: 1214–22. [CrossRef]

Shi, Enzheng, Gao Yao, Blake P. Finkenauer, Akriti, Aidan H. Coffey, and Letian Dou. 2018. Two-Dimensional Halide Perovskite Nanomaterials and Heterostructures. *Chemical Society Reviews* 47: 6001–446. [CrossRef]

Shi, Lei, Trevor L. Young, Jincheol Kim, Yun Sheng, Lei Wang, Yifeng Chen, Zhiqiang Feng, Mark J. Keevers, Xiaojing Hao, Pierre J. Verlinden, and et al. 2017. Accelerated Lifetime Testing of Organic-Inorganic Perovskite Solar Cells Encapsulated by Polyisobutylene. *ACS Applied Materials and Interfaces* 9: 25073–81. [CrossRef] [PubMed]

Shinde, Pravin S., Su Yong Lee, Jungho Ryu, Sun Hee Choi, and Jum Suk Jang. 2017. Enhanced Photoelectrochemical Performance of Internally Porous Au-Embedded α-Fe$_2$O$_3$ Photoanodes for Water Oxidation. *Chemical Communications* 53: 4278–81. [CrossRef] [PubMed]

Shlenskaya, Natalia N., Nikolai A. Belich, Michael Grätzel, Eugene A. Goodilin, and Alexey B. Tarasov. 2018. Light-Induced Reactivity of Gold and Hybrid Perovskite as a New Possible Degradation Mechanism in Perovskite Solar Cells. *Journal of Materials Chemistry A* 6: 1780–86. [CrossRef]

Singh, David J., and Ichiro Terasaki. 2008. Thermoelectrics: Nanostructuring and More. *Nature Materials* 7: 616–17. [CrossRef]

Sivula, Kevin, Florian Le Formal, and Michael Grätzel. 2011. Solar Water Splitting: Progress Using Hematite (α-Fe$_2$O$_3$) Photoelectrodes. *ChemSusChem* 4: 432–49. [CrossRef]

Song, Zhaoning, Suneth C. Watthage, Adam B. Phillips, Brandon L. Tompkins, Randy J. Ellingson, and Michael J. Heben. 2015. Impact of Processing Temperature and Composition on the Formation of Methylammonium Lead Iodide Perovskites. *Chemistry of Materials* 27: 4612–19. [CrossRef]

Souza, Flavio L., Kirian P. Lopes, Pedro A. P. Nascente, and Edson R. Leite. 2009. Nanostructured Hematite Thin Films Produced by Spin-Coating Deposition Solution: Application in Water Splitting. *Solar Energy Materials and Solar Cells* 93: 362–68. [CrossRef]

Stewart, Robert J., Christopher Grieco, Alec V. Larsen, Joshua J. Maier, and John B. Asbury. 2016. Approaching Bulk Carrier Dynamics in Organo-Halide Perovskite Nanocrystalline Films by Surface Passivation. *The Journal of Physical Chemistry Letters* 7: 1148–53. [CrossRef]

Svanström, Sebastian, T. Jesper Jacobsson, Gerrit Boschloo, Erik M. J. Johansson, Håkan Rensmo, and Ute B. Cappel. 2020. Degradation Mechanism of Silver Metal Deposited on Lead Halide Perovskites. *ACS Applied Materials and Interfaces* 12: 7212–21. [CrossRef]

Tamirat, Andebet Gedamu, John Rick, Amare Aregahegn Dubale, Wei Nien Su, and Bing Joe Hwang. 2016. Using Hematite for Photoelectrochemical Water Splitting: A Review of Current Progress and Challenges. *Nanoscale Horizons* 1: 243–67. [CrossRef]

Tan, Chih Shan, Yi Hou, Makhsud I. Saidaminov, Andrew Proppe, Yu Sheng Huang, Yicheng Zhao, Mingyang Wei, Grant Walters, Ziyun Wang, Yongbiao Zhao, and et al. 2020. Heterogeneous Supersaturation in Mixed Perovskites. *Advanced Science* 7: 1903166. [CrossRef] [PubMed]

Tee, Si Yin, Khin Yin Win, Wee Siang Teo, Leng Duei Koh, Shuhua Liu, Choon Peng Teng, and Ming Yong Han. 2017. Recent Progress in Energy-Driven Water Splitting. *Advanced Science* 4: 1600337. [CrossRef] [PubMed]

Thomson, Stuart. 2018. *Observing Phase Transitions in a Halide Perovskite Using Temperature Dependent Photoluminescence Spectroscopy*. Livingston: Edinburgh Instruments, AN_P45.

Tsege, Ermias Libnedengel, Timur Sh Atabaev, Md Ashraf Hossain, Dongyun Lee, Hyung Kook Kim, and Yoon Hwae Hwang. 2016. Cu-Doped Flower-like Hematite Nanostructures for Efficient Water Splitting Applications. *Journal of Physics and Chemistry of Solids* 98: 283–89. [CrossRef]

Turren-Cruz, Silver Hamill, Anders Hagfeldt, and Michael Saliba. 2018. Methylammonium-Free, High-Performance, and Stable Perovskite Solar Cells on a Planar Architecture. *Science* 362: 449–53. [CrossRef] [PubMed]

Uratani, Hiroki, and Koichi Yamashita. 2017. Charge Carrier Trapping at Surface Defects of Perovskite Solar Cell Absorbers: A First-Principles Study. *The Journal of Physical Chemistry Letters* 8: 742–46. [CrossRef]

Vidal, Rosario, Jaume-Adrià Alberola-Borràs, Núria Sánchez-Pantoja, and Iván Mora-Seró. 2021. Comparison of Perovskite Solar Cells with Other Photovoltaics Technologies from the Point of View of Life Cycle Assessment. *Advanced Energy and Sustainability Research* 2: 2000088. [CrossRef]

Wang, Jie, Xiaolian Chen, Fangyuan Jiang, Qun Luo, Lianping Zhang, Mingxi Tan, Menglan Xie, Yan-Qing Li, Yinhua Zhou, Wenming Su, and et al. 2018. Electrochemical Corrosion of Ag Electrode in the Silver Grid Electrode-Based Flexible Perovskite Solar Cells and the Suppression Method. *Solar RRL* 2: 1800118. [CrossRef]

Wang, Lei, Xuemei Zhou, Nhat Truong Nguyen, and Patrik Schmuki. 2015. Plasmon-Enhanced Photoelectrochemical Water Splitting Using Au Nanoparticles Decorated on Hematite Nanoflake Arrays. *ChemSusChem* 8: 618–22. [CrossRef]

Wang, Songcan, Jung Ho Yun, and Lianzhou Wang. 2017. Nanostructured Semiconductors for Bifunctional Photocatalytic and Photoelectrochemical Energy Conversion. *Semiconductors and Semimetals* 97: 315–47. [CrossRef]

Wu, Shaohang, Rui Chen, Shasha Zhang, B. Hari Babu, Youfeng Yue, Hongmei Zhu, Zhichun Yang, Chuanliang Chen, Weitao Chen, Yuqian Huang, and et al. 2019. A Chemically Inert Bismuth Interlayer Enhances Long-Term Stability of Inverted Perovskite Solar Cells. *Nature Communications* 10: 1–11. [CrossRef]

Wu, Wu-qiang, Peter N. Rudd, Zhenyi Ni, Charles Henry Van Brackle, Haotong Wei, Qi Wang, Benjamin R. Ecker, Yongli Gao, and Jinsong Huang. 2020. Reducing Surface Halide Deficiency for Efficient and Stable Iodide- Based Perovskite Solar Cells. *Journal of the American Chemical Society* 142: 3989–96. [CrossRef] [PubMed]

Wu, Yinghui, Dong Wang, Jinyuan Liu, and Houzhi Cai. 2021. Review of Interface Passivation of Perovskite Layer. *Nanomaterials* 11: 1–19. [CrossRef] [PubMed]

Xi, Lifei, and Kathrin M. Lange. 2018. Surface Modification of Hematite Photoanodes for Improvement of Photoelectrochemical Performance. *Catalysts* 8: 497. [CrossRef]

Xie, Yiyuan, Yang Ju, Yuhki Toku, and Yasuyuki Morita. 2018. Synthesis of a Single-Crystal Fe_2O_3 Nanowire Array Based on Stress-Induced Atomic Diffusion Used for Solar Water Splitting. *Royal Society Open Science* 5: 172126. [CrossRef]

Xu, Ming, Jing Feng, Xia Li Ou, Zhen Yu Zhang, Yi Fan Zhang, Hai Yu Wang, and Hong Bo Sun. 2016. Surface Passivation of Perovskite Film by Small Molecule Infiltration for Improved Efficiency of Perovskite Solar Cells. *IEEE Photonics Journal* 8: 1–7. [CrossRef]

Yan, Keyou, Yongcai Qiu, Shuang Xiao, Junbo Gong, Shenghe Zhao, Jiantie Xu, Xiangyue Meng, Shihe Yang, and Jianbin Xu. 2017. Self-Driven Hematite-Based Photoelectrochemical Water Splitting Cells with Three-Dimensional Nanobowl Heterojunction and High-Photovoltage Perovskite Solar Cells. *Materials Today Energy* 6: 128–35. [CrossRef]

Yang, Dongwen, Wenmei Ming, Hongliang Shi, Lijun Zhang, and Mao-Hua Du. 2016. Fast Diffusion of Native Defects and Impurities in Perovskite Solar Cell Material $CH_3NH_3PbI_3$. *Chemistry of Materials* 28: 4349–57. [CrossRef]

Yang, Woon Seok, Byung-Wook Park, Eui Hyuk Jung, and Nam Joong Jeon. 2017a. Iodide Management in Formamidinium-Lead-Halide–Based Perovskite Layers for Efficient Solar Cells. *Science* 356: 1376–791. [CrossRef]

Yang, Wooseok, Rajiv Ramanujam Prabhakar, Jeiwan Tan, S. David Tilley, and Jooho Moon. 2019. Strategies for Enhancing the Photocurrent, Photovoltage, and Stability of Photoelectrodes for Photoelectrochemical Water Splitting. *Chemical Society Reviews* 48: 4979–5015. [CrossRef]

Yang, Ye, Mengjin Yang, David T. Moore, Yong Yan, Elisa M. Miller, Kai Zhu, and Matthew C. Beard. 2017b. Top and bottom surfaces limit carrier lifetime in lead iodide perovskite films. *Nature Energy* 2: 1–7. [CrossRef]

Yilmaz, Ceren, and Ugur Unal. 2016. Morphology and Crystal Structure Control of α-Fe_2O_3 Films by Hydrothermal-Electrochemical Deposition in the Presence of Ce^{3+} and/or Acetate, F^- Ions. *RSC Advances* 6: 8517–27. [CrossRef]

Yun, Jae Sung, Jincheol Kim, Trevor Young, Robert J. Patterson, Dohyung Kim, Jan Seidel, Sean Lim, Martin A. Green, Shujuan Huang, and Anita Ho-Baillie. 2018. Humidity-Induced Degradation via Grain Boundaries of $HC(NH_2)_2PbI_3$ Planar Perovskite Solar Cells. *Advanced Functional Materials* 28: 1705363. [CrossRef]

Zhang, Chengxi, Dai-bin Kuang, and Wu-Qiang Wu. 2020. A Review of Diverse Halide Perovskite Morphologies for Efficient Optoelectronic Applications. *Small Methods* 4: 1900662. [CrossRef]

Zhang, Hong, Mohammad Khaja Nazeeruddin, and Wallace C. H. Choy. 2019a. Perovskite Photovoltaics: The Significant Role of Ligands in Film Formation, Passivation, and Stability. *Advanced Materials* 31: 1–29. [CrossRef] [PubMed]

Zhang, Moyao, Qi Chen, Rongming Xue, Yu Zhan, Cheng Wang, Junqi Lai, Jin Yang, Hongzhen Lin, Jianlin Yao, Yaowen Li, and et al. 2019b. Reconfiguration of Interfacial Energy Band Structure for High-Performance Inverted Structure Perovskite Solar Cells. *Nature Communications* 10: 1–9. [CrossRef] [PubMed]

Zhang, Rong, Yiyu Fang, Tao Chen, Fengli Qu, Zhiang Liu, Gu Du, Abdullah M. Asiri, Tao Gao, and Xuping Sun. 2017. Enhanced Photoelectrochemical Water Oxidation Performance of Fe_2O_3 Nanorods Array by S Doping. *ACS Sustainable Chemistry and Engineering* 5: 7502–6. [CrossRef]

Zhang, Yong, Licheng Tan, Qingxia Fu, Lie Chen, Ting Ji, and Yiwang Chen. 2016a. Enhancing the grain size of organic halide perovskites by sulfonate-carbon nanotube incorporation in high performance perovskite solar cells. *Chemical Communications* 52: 5674–77. [CrossRef]

Zhang, Yuchao, Hongwei Ji, Wanhong Ma, Chuncheng Chen, Wenjing Song, and Jincai Zhao. 2016b. Doping-Promoted Solar Water Oxidation on Hematite Photoanodes. *Molecules* 21: 868. [CrossRef]

Zhang, Yuchao, Shiqi Jiang, Wenjing Song, Peng Zhou, Hongwei Ji, Wanhong Ma, Weichang Hao, Chuncheng Chen, and Jincai Zhao. 2015. Nonmetal P-Doped Hematite Photoanode with Enhanced Electron Mobility and High Water Oxidation Activity. *Energy and Environmental Science* 8: 1231–36. [CrossRef]

Zhao, Jingjing, Xiaopeng Zheng, Yehao Deng, Tao Li, Yuchuan Shao, Alexei Gruverman, Jeffrey Shield, and Jinsong Huang. 2016a. Is Cu a Stable Electrode Material in Hybrid Perovskite Solar Cells for a 30-Year Lifetime? *Energy and Environmental Science* 9: 3650–56. [CrossRef]

Zhao, Lianfeng, Ross A. Kerner, Zhengguo Xiao, Yunhui Lisa, Kyung Min Lee, Jeffrey Schwartz, Barry P. Rand, and Barry P. Rand. 2016b. Redox Chemistry Dominates the Degradation and Decomposition of Metal Halide Perovskite Optoelectronic Devices Redox Chemistry Dominates the Degradation and Decomposition of Metal Halide Perovskite Optoelectronic Devices. *ACS Energy Letters* 1: 595–602. [CrossRef]

Zhao, Yi Cheng, Wen Ke Zhou, Xu Zhou, Kai Hui Liu, Da Peng Yu, and Qing Zhao. 2017. Quantification of Light-Enhanced Ionic Transport in Lead Iodide Perovskite Thin Films and Its Solar Cell Applications. *Light: Science and Applications* 6: e16243. [CrossRef] [PubMed]

Zheng, Haiying, Guozhen Liu, Liangzheng Zhu, Jiajiu Ye, Xuhui Zhang, Ahmed Alsaedi, Tasawar Hayat, Xu Pan, and Songyuan Dai. 2018. The Effect of Hydrophobicity of Ammonium Salts on Stability of Quasi-2D Perovskite Materials in Moist Condition. *Advanced Energy Materials* 8: 1–8. [CrossRef]

Zheng, Kaibo, and Tönu Pullerits. 2019. Two Dimensions Are Better for Perovskites. *Journal of Physical Chemistry Letters* 10: 5881–85. [CrossRef]

Zheng, Xiaopeng, Joel Troughton, Nicola Gasparini, Yuanbao Lin, Mingyang Wei, Yi Hou, Jiakai Liu, Kepeng Song, Zhaolai Chen, Chen Yang, and et al. 2019. Quantum Dots Supply Bulk- and Surface-Passivation Agents for Efficient and Stable Perovskite Solar Cells. *Joule* 3: 1963–76. [CrossRef]